

Interactive Effects of Salinity, Redox State, Soil Type, and Colloidal Size Fractionation on Greenhouse Gas Production in Coastal Wetland Soils

Nicholas D Ward¹, Madison Bowe¹, Katherine A Muller¹, Xingyuan Chen², Qian Zhao¹, Rosalie Chu³, Zezhen Cheng³, Thomas W. Wietsma², and Ravi K Kukkadapu¹

¹Pacific Northwest National Laboratory

²Pacific Northwest National Laboratory (DOE)

³PNNL

December 3, 2023

Abstract

This study examines how greenhouse gas (GHG) production and organic matter (OM) transformations in coastal wetland soils vary with the availability of oxygen and other terminal electron acceptors. We also evaluated how OM and redox-sensitive species varied across different size fractions: particulates (0.45-1 μ m), fine colloids (0.1-0.45 μ m), and nano particulates plus truly soluble (<0.1 μ m; NP+S) during 21-day aerobic and anaerobic slurry incubations. Soils were collected from the center of a freshwater coastal wetland (FW-C) in Lake Erie, the upland-wetland edge of the same wetland (FW-E), and the center of a saline coastal wetland (SW-C) in Washington state. Anaerobic methane production for FW-E soils were 47 and 27,537 times greater than FW-C and SW-C soils, respectively. High particulate Fe²⁺ and dissolved sulfate concentrations in FW-C and SW-C soils suggest that iron and/or sulfate reduction inhibited methanogenesis. Aerobic CO₂ production was highest for both freshwater soils, which had a higher proportion of OM in the NP+S fraction (64 \pm 28% and 70 \pm 10% for FW-C and FW-E, respectively) and C:N ratios reflective of microbial detritus (1.7 \pm 0.2 and 1.4 \pm 0.3 for FW-E and FW-C, respectively) compared to SW-C, which had a higher fraction of particulate (58 \pm 9%) and fine colloidal (19 \pm 7%) OM and C:N ratios reflective of vegetation detritus (11.2 \pm 0.5). The variability in GHG production and shifts in OM size fractionation and composition observed across freshwater and saline soils collected within individual and across different sites reinforce the high spatial variability in the processes controlling OM stability, mobility, and bioavailability in coastal wetland soils.

Hosted file

980205_0_art_file_11621074_s4jqds.docx available at <https://authorea.com/users/553153/articles/689538-interactive-effects-of-salinity-redox-state-soil-type-and-colloidal-size-fractionation-on-greenhouse-gas-production-in-coastal-wetland-soils>

Hosted file

980205_0_supp_11621077_s4jqds.docx available at <https://authorea.com/users/553153/articles/689538-interactive-effects-of-salinity-redox-state-soil-type-and-colloidal-size-fractionation-on-greenhouse-gas-production-in-coastal-wetland-soils>

1
2 **Interactive Effects of Salinity, Redox State, Soil Type, and Colloidal Size**
3 **Fractionation on Greenhouse Gas Production in Coastal Wetland Soils**

4
5 **N. D Ward^{1-2*†}, M. Bove^{1†}, K. A. Muller³, X. Chen³, Q. Zhao³, R. Chu³, Z. Cheng³, T.**
6 **Wietsma³, and R. K. Kukkadapu³**

7 ¹Pacific Northwest National Laboratory, Sequim WA, 98382

8 ²School of Oceanography, University of Washington, Seattle, WA 98105, USA

9 ³Pacific Northwest National Laboratory, Richland, WA 99352, USA

10
11 *Corresponding author: Nicholas Ward (nicholas.ward@pnl.gov)

12 †Contributed equally

13
14 **Key Points:**

- 15 • Sulfur and/or iron reduction limited anaerobic methane production in two of the three
16 incubated freshwater and saline coastal soils
- 17 • Aerobic respiration was highest in soil with carbon composed of microbial detritus and a
18 greater fraction of soluble vs. colloidal carbon
- 19 • Particulates and colloids comprised a major fraction of the saline soil's mobile carbon
20 pool (58±9% and 19±7%, respectively)

21 **Abstract**

22 This study examines how greenhouse gas (GHG) production and organic matter (OM)
23 transformations in coastal wetland soils vary with the availability of oxygen and other terminal
24 electron acceptors. We also evaluated how OM and redox-sensitive species varied across
25 different size fractions: particulates (0.45-1 μ m), fine colloids (0.1-0.45 μ m), and nano particulates
26 plus truly soluble (<0.1 μ m; NP+S) during 21-day aerobic and anaerobic slurry incubations. Soils
27 were collected from the center of a freshwater coastal wetland (FW-C) in Lake Erie, the upland-
28 wetland edge of the same wetland (FW-E), and the center of a saline coastal wetland (SW-C) in
29 Washington state. Anaerobic methane production for FW-E soils were 47 and 27,537 times
30 greater than FW-C and SW-C soils, respectively. High particulate Fe²⁺ and dissolved sulfate
31 concentrations in FW-C and SW-C soils suggest that iron and/or sulfate reduction inhibited
32 methanogenesis. Aerobic CO₂ production was highest for both freshwater soils, which had a
33 higher proportion of OM in the NP+S fraction (64 \pm 28% and 70 \pm 10% for FW-C and FW-E,
34 respectively) and C:N ratios reflective of microbial detritus (1.7 \pm 0.2 and 1.4 \pm 0.3 for FW-E and
35 FW-C, respectively) compared to SW-C, which had a higher fraction of particulate (58 \pm 9%) and
36 fine colloidal (19 \pm 7%) OM and C:N ratios reflective of vegetation detritus (11.2 \pm 0.5). The
37 variability in GHG production and shifts in OM size fractionation and composition observed
38 across freshwater and saline soils collected within individual and across different sites reinforce
39 the high spatial variability in the processes controlling OM stability, mobility, and bioavailability
40 in coastal wetland soils.

41

42 **Plain Language Summary**

43 Coastal wetlands, including freshwater systems near large lakes, rapidly bury carbon, but less is
44 known about how they transport carbon either to marine/lake environments or to the atmosphere
45 as greenhouse gases such as carbon dioxide and methane. Coastal wetlands face multiple threats
46 that may alter how they cycle carbon such as sea level rise and lake level variability. We
47 performed experiments on saline and freshwater coastal soils with and without oxygen present to
48 understand what chemical factors drove greenhouse gas production. We also examined the
49 different forms and size classes of carbon released from the soils when inundated and found that
50 colloids, an understudied “solid” form of carbon smaller than particles but bigger than dissolved
51 carbon, can represent anywhere from 1-44% of the total carbon released depending on soil type
52 and oxygen availability. We also found that methane production in the absence of oxygen was
53 nearly 28,000 times greater in a freshwater wetland soil compared to a saline soil that had
54 competing reactions occurring such as iron and sulfur utilization. Carbon dioxide production in
55 the presence of oxygen was greatest for samples with the highest proportion of carbon in the
56 dissolved size fraction compared to larger colloids and particles.

57 **1 Introduction**

58 Vegetated coastal systems play a disproportionate role in carbon cycling compared to their land
59 cover area, as they occupy only 0.07-0.22% of Earth’s surface, yet account for approximately 10%
60 of the net residual land C sequestration (Spivak et al. 2019). Accordingly, coastal wetlands are an
61 area of significant interest in discussions of climate mitigation and solutions (Moomaw et al.
62 2018, Villa & Bernal 2018, Wang et al. 2019), though we currently lack a predictive

63 understanding of the complex and changing controls of carbon cycling in these dynamic systems
64 (Ward et al. 2020). Increasing global temperatures are expected to alter wetland carbon storage
65 via both enhanced productivity and decomposition (Kirwan & Blum 2011, Olsson et al. 2015),
66 though this effect may be limited in colder environments (Sjögersten et al. 2014). In addition to
67 the direct effects of rising temperatures, climate change and associated phenomena including
68 relative sea level rise (SLR), lake level variability along large freshwater coastlines, and
69 increasing occurrence and severity of extreme weather events like storm surge and hurricanes are
70 predicted to increase the exposure of coastal systems to seawater and rainfall flooding (Tully et
71 al. 2019, Wuebbles et al. 2019, Lønborg et al. 2020). These hydrological disturbances are
72 expected to impact biogeochemical processing, with effects varying between wetlands of
73 differing salinities, elevations, flooding frequency, and other antecedent conditions (Clark et al.
74 2007, Altor & Mitsch 2008, Noe et al. 2013, Stagg et al. 2017; Sengupta et al., 2021).

75 Soil as a dynamic organic matter (OM) pool is a crucial component of the global carbon cycle
76 (Stockmann et al. 2013, Rodrigo-Comino et al. 2020, Lal et al. 2021). Likewise, the quantity and
77 quality of carbon exported laterally from coastal wetlands is poorly quantified and may serve as
78 an important, but under examined carbon sink (Santos et al. 2021). Soil OM in the aqueous phase
79 can transition between particulate, colloidal, and dissolved forms in soil and may be stabilized or
80 transported out of soil—a fate that is influenced by a complex mixture of factors (Marín-Spiotta
81 et al. 2014). Anoxic conditions have been shown to promote dissolved organic carbon (DOC)
82 release from soil in nitrate-reducing conditions, but markedly decrease DOC release under
83 sulfate-reducing and methanogenic conditions (Kim & Pfaender 2005). Other work has found
84 increased DOC release under reducing conditions due to associated pH increases and reduction
85 of reactive iron and manganese (Grybos et al. 2009). Increased salinity is also thought to induce
86 flocculation of OM, particularly humic substances, and inhibit extraction of OM from soils (Kida
87 et al. 2017). The complexities of how soil OM fractionates across different size fractions, and the
88 relative reactivity of these fractions, is not currently considered in our understanding of lateral
89 carbon export from coastal wetlands (Maher et al. 2013, Ho et al. 2017, Chu et al. 2018)

90 In addition to export out of wetland soils, OM can be decomposed in soil and yield greenhouse
91 gas (GHG) release, the rate of which is also influenced by a combination of environmental,
92 geochemical, mineralogical, and microbial factors (Schmidt et al., 2011; Patel et al., 2022).
93 Reducing conditions lower decomposition rates via a hypothesized mechanism referred to as the
94 “enzymic latch,” in which anoxia inhibits the activity of phenol oxidase enzymes (Freeman et al.
95 2001). More recently Wang et al. (2017) have implicated iron oxidation in regulating phenol
96 oxidation activity in oxic conditions and counteracting the “latching” effect of oxygen to phenol
97 oxidases. Though in oxic soils iron (hydr)oxides contribute to OM storage (Wagai & Mayer
98 2007), in anoxic conditions iron hydroxides acting as terminal electron acceptors can increase
99 OM decomposition (Buettner et al. 2014, Chen et al. 2020). Observed effects of increasing
100 salinity on soil decomposition rates have varied across field and lab studies, and include
101 stimulation of decomposition (Stagg et al. 2018), inhibition (Neubauer et al. 2013, Qu et al.
102 2019, Zhang et al. 2022), stimulation of CH₄ release with inhibition of CO₂ (Zhang et al. 2022),
103 negligible methane emissions in polyhaline marshes (Poffenbarger et al. 2011), and a quadratic
104 relationship with initial decrease in decomposition with increasing salinity followed by
105 heightened decomposition at higher salinities (Stagg et al. 2017). One proposed mechanism
106 contributing to altered GHG emissions with salinity is that the sulfate found in seawater has been
107 associated with increased sulfate reduction rates (Weston et al. 2011) and thus increased CO₂

108 emissions from carbon mineralization (Feng & Hsieh 1998), though not consistently across
109 studies (Herbert et al. 2015). Sulfate exposure in wetland soils has also been observed to
110 suppress methanogenesis (Helton et al. 2019).

111 The heterogeneous nature of soil environments complicates the interpretation of the
112 biogeochemical behaviors described above. Biogeochemical processes can be highly influenced
113 by heterogenous characteristics such as soil microsites (Parkin et al., 1987) and differing pore
114 sizes (Bailey et al., 2017) among other factors. The size distribution of water-soluble OM and
115 redox-sensitive elements in soil porewaters is one such factor that might play a key role in
116 determining the mobility and/or reactivity of OM in soils. Laboratory characterizations of OM
117 often focus on DOC, operationally defined as the carbon that passes through filters ranging in
118 pore size from 0.2 to 0.7 μm ; this practice has been recently questioned due to the resulting
119 overestimation of truly soluble DOC via the inclusion of colloids (Yan et al. 2018, Afsar et al.
120 2020, 2023). The importance of understanding the role of colloids in soil carbon cycling stems in
121 part from their highly reactive surfaces that permit binding to OM (Rod et al. 2020). Thus,
122 understanding how the biogeochemical behavior of colloidal size fractions varies under different
123 environmental and mineralogical conditions is central to constraining the mechanisms underlying
124 soil OM transport and transformation.

125 Coastal wetland salinity exposure and redox conditions are predicted to change in response to
126 altered precipitation patterns, SLR, and storm surge, making an understanding of the
127 compounding effects of these disturbances on wetland soil OM transport, decomposition, and
128 storage particularly important (Spivak et al. 2019, Moomaw et al. 2018). Given the array of
129 factors influencing carbon cycling changes in coastal wetlands in response to redox shifts and
130 inundation, we sought to examine how GHG production and OM transformations in soils
131 collected from different freshwater and saline wetland settings varied under aerobic versus
132 anaerobic conditions and in the presence of other terminal electron acceptors.

133 During 21-day incubations conducted in aerobic and anaerobic conditions, we tested how oxygen
134 availability, soil origin, and inundation history influence the evolution of GHG production, bulk
135 chemical properties, redox sensitive species, and biodegradation of OM across three size
136 fractions: nano particulates plus truly soluble OM (NP+S; $< 0.1 \mu\text{m}$), fine colloids (FC; 0.1-0.45
137 μm), and particulates (P; 0.45-1 μm). We hypothesized that anaerobic methane production would
138 be outcompeted by iron or sulfate reduction for soils with exposure to high levels of either
139 aqueous or mineral-derived sulfate and iron, and that the relative proportion of soluble versus
140 mineral-associated colloidal and particulate OM would be an important factor mediating aerobic
141 respiration.

142 **2 Materials and Methods**

143 **2.1 Soil Collection**

144 Two surface soil samples were collected from a freshwater site (FW), located near the outlet of
145 Old Woman Creek into Lake Erie (Huron, Ohio, United States). These samples were collected at
146 the wetland center (i.e., in the center of the wetland, FW-C; 41.37613787°, -82.50754702°) and
147 at the upland-wetland edge (i.e., near the border between where wetland vegetation starts
148 transitioning to upland vegetation, FW-E; 41.37590722, -82.5071329°). FW-C soils are

149 characterized primarily as frequently flooded silty fluvaquents; FW-E soils are occasionally
150 flooded and characterized primarily as Holly silt loam (USDA Natural Resources Conservation
151 Service n.d.). In general, the freshwater site is characterized by surface water with salinity
152 generally between 0.1 and 0.3 PSU, and dissolved oxygen (DO) ranging from 5-15 mg/L
153 (NOAA NERRS 2022). At the time of soil collection on 12/9/2021, porewater DO was 10.5
154 mg/L at FW-E and 1.5 mg/L at the FW-C, measured using a YSI Pro Plus multiparameter sonde
155 connected to a porewater sipper rod (M.H.E. products).

156 A third sample was collected at the center of a saline wetland (SW-C) from the floodplain of
157 Beaver Creek (46.905938°, -123.978047°), a tidally influenced first-order tributary draining into
158 Johns River, which flows into the Grays Harbor estuary in Washington state. Beaver Creek
159 floodplain soils are characterized as hydric Ocosta silty clay loam (USDA Natural Resources
160 Conservation Service n.d.) and soil texture is primarily silty clay, but ranges from sandy clay
161 loam to clay (Sengupta et al., 2019). Groundwater in this floodplain is generally anaerobic and
162 has salinities between 15-30 PSU during dry periods and 5-20 PSU during wet periods (Regier et
163 al. 2021). Detailed site information is described by Yabusaki et al. (2020). When the soil was
164 collected on 1/25/2022, porewater DO was 2.2 mg/L and salinity was 3.6 PSU. All soil samples
165 were collected at approximately 30 cm depth and were stored in sealed bags at 4°C prior to
166 incubation.

167 2.2 Incubations and Greenhouse Gas Analyses

168 Prior to soil incubations, the soils were conditioned in a Coy anaerobic chamber at O₂ levels
169 below 20 ppm for four days. Vegetation and rocks were removed by hand. A subsample of each
170 soil was dried in aerobic conditions for bulk characterization [total C (TC), total nitrogen (TN),
171 and total sulfur (TS)]. Field moist soil was suspended in deoxygenated de-ionized water in 1 L
172 microcosms with ~250 mL headspace and shaken for 5 minutes, the end of which marked the
173 initial timepoint (referred to as “pre-incubation”). Soil:water weight ratios were determined by
174 drying subsamples of soils to find percent moisture and were 1:12.7 for FW-C soil, 1:16.5 for
175 FW-E soil, and 1:11.0 for SW-C soil.

176 At the initial timepoint, triplicate bottles were destructively sampled for chemical analyses. A
177 subset of bottles were incubated under anaerobic incubations; bottles were shaken within the
178 anaerobic chamber with deoxygenated water, and headspaces were purged with N₂ gas five days
179 per week following GHG sampling. Aerobic incubations were initiated by adding water with
180 ambient O₂ levels. Bottles were shaken with ambient air and the suspension was allowed to
181 equilibrate with ambient air beforehand, and headspaces were purged with room air throughout
182 the incubations. After shaking, headspaces were sampled with 60 mL syringes via lids fitted with
183 two luer valves for gas analysis, which were then sealed. Incubations were carried out in the dark
184 for 21 days at temperatures between 19-21°C before destructive sampling of soil and the
185 supernatant for a variety of size-fractionated analyses.

186 Headspace gas was sampled 5 days per week (i.e., Monday through Friday) during incubations,
187 at which point incubations were shaken vigorously for 60 seconds to homogenize and equilibrate
188 aqueous incubate with headspace. Oxygen content was measured with an optical oxygen meter to
189 confirm the extent of anoxic conditions or anoxia (Pyroscience, FireSting GO₂). Partial pressures

190 of headspace CO₂ and CH₄ were measured via a cavity ring-down spectrometer (Picarro, G2508
191 Gas Concentration Analyzer).

192 2.3 Size-fractionated Chemical Analyses

193 At the start and end of incubations, liquid suspensions were divided into 50-mL centrifuge tubes
194 and centrifuged to generate supernatants of three size fractions:

195 **(1) <1 μm** [a mixture of soluble OM (S; <10 kDa - 2.5 nm), mineral-associated nanoparticulate
196 colloids (NP; 2.5 nm - 0.1 μm), mineral-associated fine colloids (FC; 0.1 μm-0.45 μm), and
197 mineral-associated particulate organic matter (P; 0.45 μm - 1.0 μm)];

198 **(2) <0.45 μm** [a composite of soluble OM, nanoparticulate, and fine colloidal fractions (although
199 each of these fractions are present in < 0.45 μm filtered samples, this fraction is often
200 erroneously referred to as soluble dissolved organic carbon)] and;

201 **(3) <0.1 μm** (nanoparticulate and soluble OM), following the methods of Afsar et al. (2020).
202 Pre-incubation samples and anaerobic incubations were handled in an anaerobic chamber to
203 maintain anoxia prior to analyses.

204 Size-fractionated and bulk (i.e., unfiltered) pre-incubation and incubated samples were analyzed
205 on an automatic titrator (Mettler-Toledo, T7 Excellence) for pH, alkalinity, and oxidation-
206 reduction potential (ORP; Figures S1-2). Size-fractionated slurry samples were also analyzed for
207 ferrous iron (Fe²⁺) concentration by colorimetric assay (Thermo Scientific, FerroZine™ iron
208 reagent) and total iron content and abundance via ICP-OES (Perkin Elmer, Optima 7300 DV).
209 Ferrous iron concentration was analyzed using the ferrozine assay (Stookey, 1970). Briefly, 0.4
210 mL of well-mixed sample was added to 4 mL of 1 g/L ferrozine in 20 mM PIPES (piperazine-
211 1,4-bis (2-ethanesulfonic acid)) buffer at pH 7 and shaken to homogenize. After five minutes, the
212 solution was measured for the absorbance at 562 nm by an ultraviolet-visible spectrophotometer
213 (UV-Vis) (Evolution 260 BIO, Thermo Scientific).

214 Sulfate and nitrate concentrations were measured via ion chromatography (ThermoFisher,
215 Dionex ICS-6000 HPIC). Due to instrument limitations, it was not possible to analyze by size
216 fractions without damaging the instrument, so samples were filtered to 0.2 μm prior to analysis.

217 Aqueous TOC and TN concentrations were measured on size-fractionated and bulk samples on a
218 Shimadzu TOC-L. Samples were stirred via a magnetic stir bar during analysis to ensure
219 homogeneity.

220 At the start and end time points of incubations, solid soils remaining in the bottom of reactors
221 were subsampled, and soils from triplicates within treatments were homogenized together prior
222 to oven drying. The combined dry soil sample was analyzed for TC, TN, and TS (Elementar
223 vario EL Elemental Analyzer; Figures S3-5).

224 Supernatant samples were characterized by 21T Fourier transform ion cyclotron resonance mass
225 spectrometer (FTICR-MS) located at the Environmental Molecular Sciences Laboratory (
226 Richland, WA). Samples were randomized and directly infused into the FTICR-MS, after SPE
227 clean-up (Dittmar et al. 2008), via an automated direct infusion cart (Orton et al. 2018). Samples

228 were measured in negative electrospray ionization (-ESI) polarity with technical replicates. All
229 spectra were peak picked, internally calibrated and chemical formulae assigned using
230 Formularity (Tolić et al. 2017) considering only the presence of C, H, O, N, S and P.

231 2.4 Data Analysis

232 The concentration of CO₂ and CH₄ in the headspace and dissolved in incubates were calculated
233 using Henry's law, the ideal gas law, and temperature-dependent coefficients from Weiss (1974),
234 Wiesenburg & Guinasso (1979), and Weiss & Price (1980). See Magen et al. (2014) for relevant
235 equations. Cumulative moles of each gas produced during incubations were determined by
236 correcting for gas removed during sampling and added during headspace purging. The room air
237 used to purge the aerobic incubations after each gas sampling was measured with the cavity ring-
238 down spectrometer (Picarro, G2508 Gas Concentration Analyzer) so that the amount of CO₂ and
239 CH₄ added to the headspace was known.

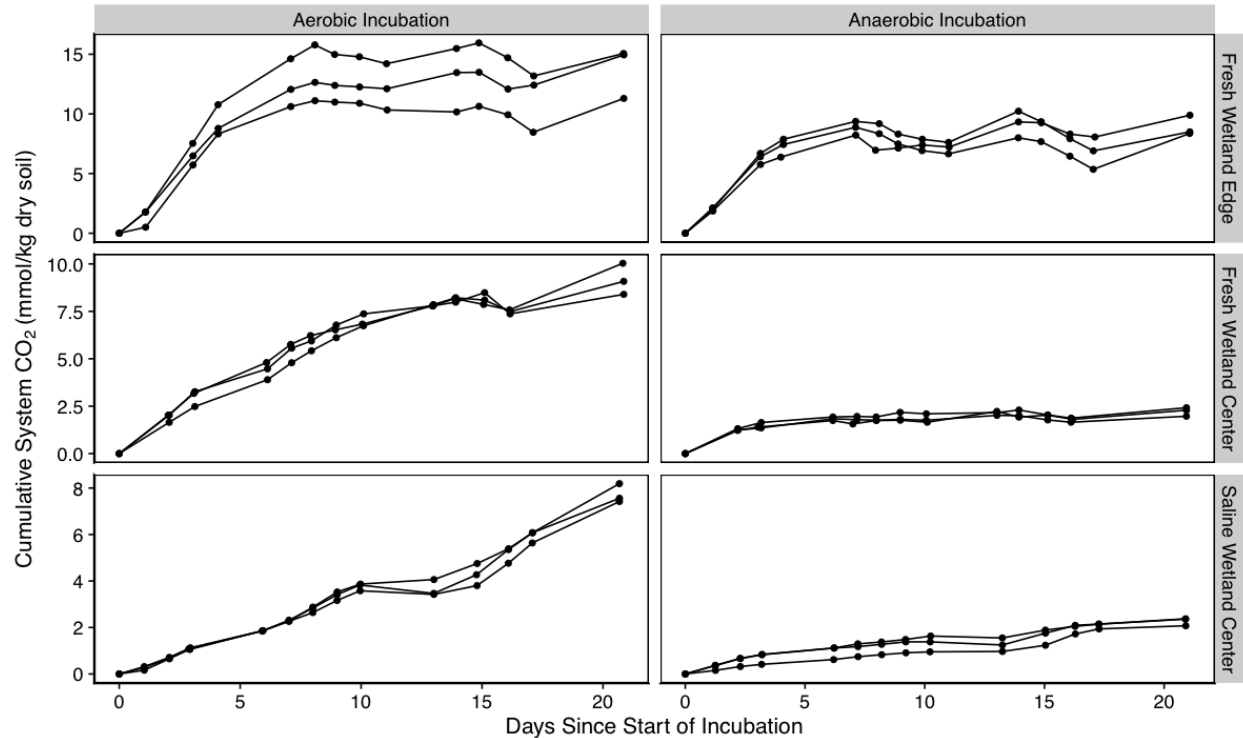
240 Chemical concentrations in each individual colloidal size fraction (e.g., <0.1 μm, 0.1-0.45, and
241 0.45-1 μm) were calculated by subtraction. TOC, TN, and Fe²⁺ concentrations in the largest size
242 fraction (0.45-1 μm, or OM solely associated with particulates referred to as "P" throughout)
243 were deduced by subtracting data from the <0.45 μm samples. Size-fractionated values for the
244 medium-size fractions (0.1-0.45 μm, or solely fine colloids, referred to as "FC" throughout) were
245 determined by subtracting values from the <0.1 μm (smallest size; composite of nanoparticulates
246 and truly soluble OM, referred to as "NP+S" throughout) samples from those of the <0.45 μm
247 samples. C:N ratios were calculated for aqueous samples using TOC and TN values and were
248 calculated for solid soils using TC and TN data.

249 All statistical analyses were performed in the statistical computing language R using R Studio
250 version 2023.09.0+463 (RStudio Team, 2020). Paired t-tests, using Benjamini & Hochberg p
251 value adjustment were used to compare significant differences in chemical concentrations
252 between pre- and post-incubation samples, incubation types, soil types, and size fractions.
253 Reported p values represent comparisons of one group to another. Significant differences were
254 considered to fall within a 95% confidence interval (i.e., $p < 0.05$). Pearson correlation was used
255 to compare linearity in GHG production rates across the different experiments.

256 3 Results

257 3.1 Greenhouse Gas Production

258 First, we describe how GHG production varied across the different soil types and incubation
259 conditions. After 21 days under aerobic conditions, the FW-C and SW-C soils produced similar
260 amounts of CO₂ (9.17 ± 0.82 and 7.72 ± 0.41 mmol C / kg dry soil by the end of the experiment,
261 respectively; $p > 0.05$), whereas the FW-E soils produced significantly more CO₂ by day 21 of
262 the incubation (13.8 ± 2.14 mmol C / kg dry soil; $p < 0.05$). In addition to the FW-E soils
263 producing more CO₂ under aerobic conditions, the rate of CO₂ production peaked after seven
264 days (Figure 1), resulting in a less linear behavior over the course of the 21-day incubation ($R^2 =$
265 0.72) compared to FW-C ($R^2 = 0.94$) and SW-C soils ($R^2 = 0.98$).



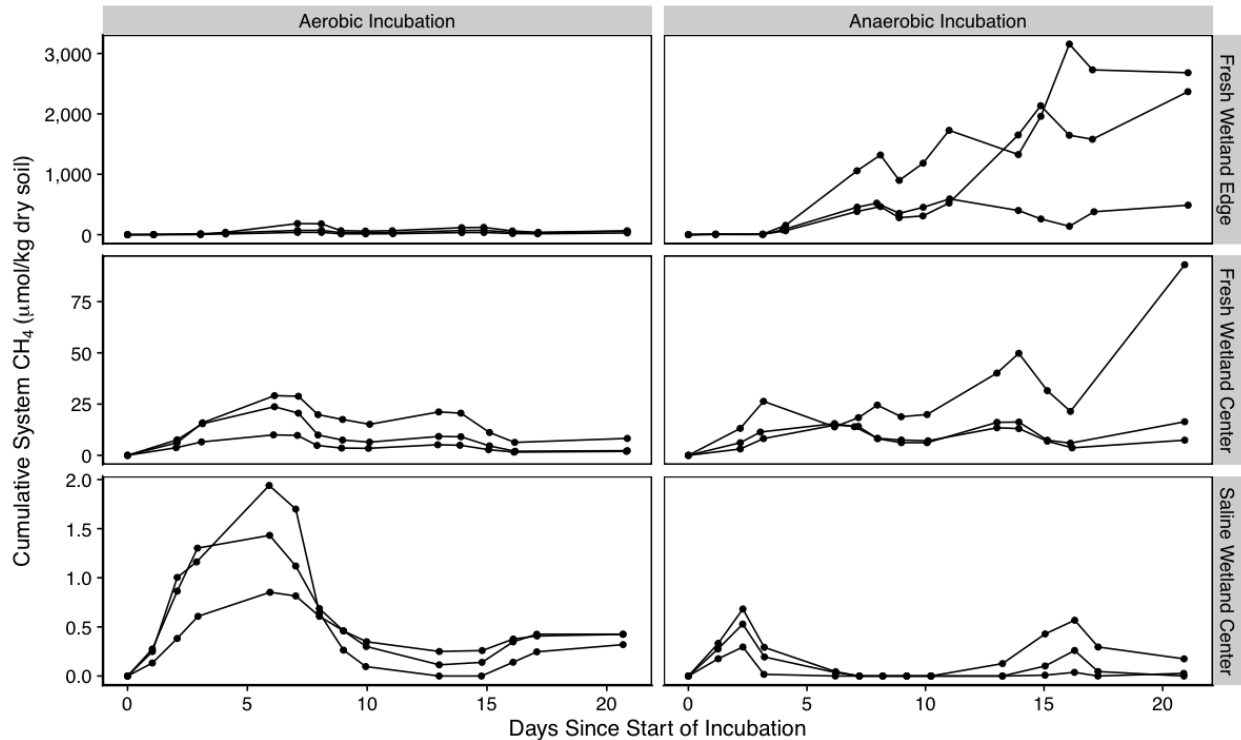
266

267 **Figure 1.** Net carbon dioxide production during incubations expressed per kg of dry soil. Note
 268 that y-axis scaling varies between top, middle, and bottom panels to allow trends to be seen more
 269 clearly.

270 For all three types of soils, total CO₂ production over the 21-day experiment was lower under
 271 anaerobic conditions compared to the same soil incubated under aerobic conditions. Aerobic CO₂
 272 production was 4.1, 1.5, and 3.4 times greater than anaerobic production for FW-C, FW-E, and
 273 SW-C soils, respectively ($p < 0.05$). Likewise, when considering all soil types together, the
 274 aerobic experiments produced 2.3 times more CO₂ than the anaerobic experiments at the end of
 275 the experiment ($p < 0.05$). As with the aerobic experiments, after 21 days under anaerobic
 276 conditions, the FW-C and SW-C soils produced similar amounts of CO₂ (2.22 ± 0.23 and $2.27 \pm$
 277 0.17 mmol C / kg dry soil, respectively; $p > 0.05$), whereas the FW-E soils produced
 278 significantly more CO₂ (8.92 ± 0.85 mmol C / kg dry soil; $p < 0.05$). The temporal behavior of
 279 CO₂ production observed in the anaerobic experiments (Figure 1) were similar to the aerobic
 280 experiments with FW-E peaking around day 4 and exhibiting the least linear behavior ($R^2 =$
 281 0.66) compared to FW-C ($R^2 = 0.73$) and SW-C ($R^2 = 0.93$).

282 A small, but negligible amount of CH₄ production was detected for all three soil types under
 283 aerobic conditions (Figure 2). After 21 days under aerobic conditions, SW-C soils produced the
 284 least CH₄ (0.390 ± 0.061 μ mol C / kg dry soil), followed by FW-C (4.16 ± 3.56 μ mol C / kg dry
 285 soil), and FW-E (49.7 ± 47.0 μ mol C / kg dry soil). Similar to CO₂ production, the difference in
 286 aerobic methane production was significant between FW-E and the other two soil types ($p <$
 287 0.05), whereas FW-C and SW-C were not significantly different ($p > 0.05$).

288



289

290 **Figure 2.** Net methane production during incubations expressed per kg of dry soil. Note that y-
 291 axis scaling varies between top, middle, and bottom panels to allow trends to be seen more
 292 clearly.

293 The minimal methane production under aerobic conditions was to be expected; however,
 294 interestingly, even under anaerobic conditions CH_4 production was low for FW-C and SW-C
 295 soils (38.9 ± 47.0 and 0.067 ± 0.094 $\mu\text{mol C} / \text{kg dry soil}$ by the end of the incubation,
 296 respectively), suggesting that other redox processes inhibited methanogenesis during the
 297 incubations (Figure 2). In contrast, FW-E soils had substantially higher amounts of CH_4 ($p <$
 298 0.05) produced after 21 days ($1,845 \pm 1,186$ $\mu\text{mol C} / \text{kg dry soil}$) with methane production not
 299 initiating until day four. It is possible that methane production may have occurred in the FW-C
 300 and SW-C soils if incubated longer, allowing other terminal electron acceptors to be exhausted.

301 The molar ratio of $\text{CO}_2:\text{CH}_4$ varied substantially between incubation conditions, ranging from a
 302 minimum value of 2.51 in the FW-E anaerobic experiment to a maximum value of 225,206 in the
 303 SW-C anaerobic experiment (Figure S6). The average $\text{CO}_2:\text{CH}_4$ ratio for the final time point
 304 (day 21) of the anaerobic experiments was lowest for FW-E (8.98 ± 9.76), followed by FW-C
 305 (152 ± 144) and SW-C ($49,295 \pm 52,940$); despite the large differences in mean ratios at the end
 306 of the experiment, differences between soil types were not significant given the large variability
 307 between triplicates ($p > 0.05$). The average $\text{CO}_2:\text{CH}_4$ ratio for the final time point (day 21) of the
 308 aerobic experiments was similarly lowest in the FW-E soils (299 ± 89.5), followed by FW-C
 309 ($3,386 \pm 2,134$) and SW-C ($20,121 \pm 3,186$); in this case there was a significant difference
 310 between SW-C and FW-E ($p < 0.05$).

311 3.2 Physiochemical Conditions of the Incubations

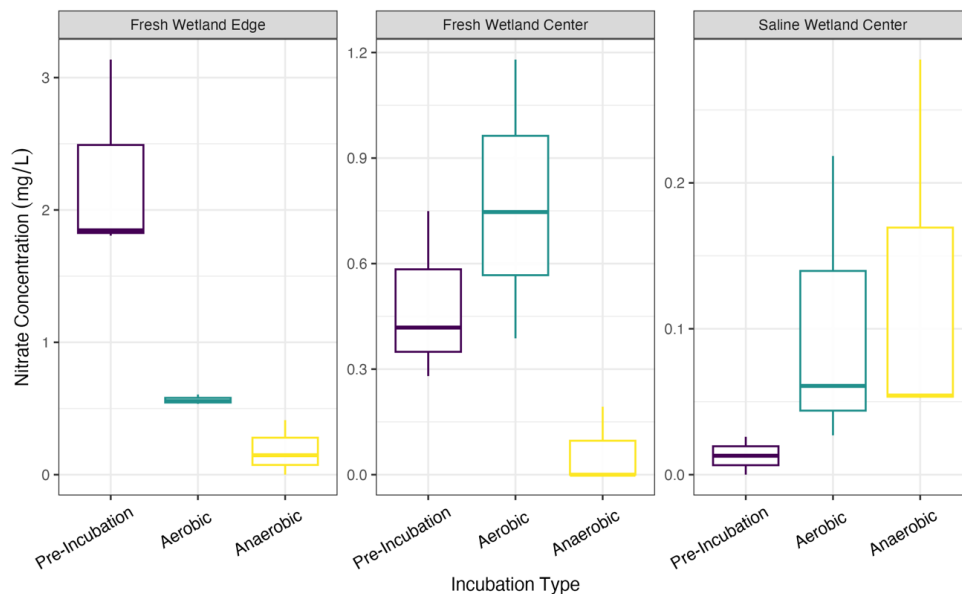
312 To contextualize the physiochemical conditions each soil experienced during the incubations, we
313 first examine changes in ORP, pH, and alkalinity. ORP of all size ranges of both freshwater
314 wetland soils increased after being incubated under aerobic conditions for 21 days (Figure S1).
315 In contrast, ORP decreased, albeit to a smaller degree, in the saline samples under both aerobic
316 and anaerobic conditions (Figure S1). The observed increase in ORP for freshwater samples
317 incubated under aerobic conditions was significant ($p < 0.05$) for all size fractions except for the
318 bulk size fraction for FW-E, the $<1 \mu\text{m}$ size fraction for FW-C soils, and the $<0.45 \mu\text{m}$ size
319 fraction for FW-E soils ($p > 0.05$). The decrease in ORP under aerobic conditions observed for
320 SW-C was significant ($p > 0.05$) for all size fractions except for the bulk unfiltered sample ($p >$
321 0.05). Under anaerobic conditions, ORP decreased for all the size ranges in FW-C and SW-C
322 incubates but was marginally higher for the FW-E soils. These differences were statistically
323 significant except for the $<1 \mu\text{m}$ size fraction for FW-C soils, $<0.45 \mu\text{m}$ size fraction for FW-E
324 soils, and $<0.1 \mu\text{m}$ size fraction for FW-C soils. ORP reached negative values in all but the
325 smallest size fraction ($<0.1 \mu\text{m}$) for SW-C soils.

326 Alkalinity of the incubated solutions was measured to understand differences in cation and
327 carbonate/bicarbonate exchange between the soil matrix and each size fraction. Alkalinity
328 increased in all three soil types after being incubated under anaerobic conditions ($p < 0.05$).
329 Alkalinity also increased in all soils and size fractions under aerobic conditions, but to a smaller
330 extent (Figure S1); these changes were statistically significant in all cases except for the bulk and
331 $<0.1 \mu\text{m}$ size fraction for FW-E soils ($p < 0.05$). pH was generally higher in the anaerobic
332 incubations compared to aerobic and ranged from 6.0 to 7.7 across all size fractions, soil types,
333 and incubation conditions (Figure S2).

334 3.3 Competing Redox Reactions

335 Next, we examine how a variety of redox-sensitive elements evolved throughout the incubations,
336 possibly influencing the observed trends in GHG production particularly in the anaerobic
337 incubations where O_2 was not available as a terminal electron acceptor. We also assess how each
338 parameter is speciated across different size fractions (when analytically feasible) to understand
339 the dominant forms found across the studied soil types and redox states.

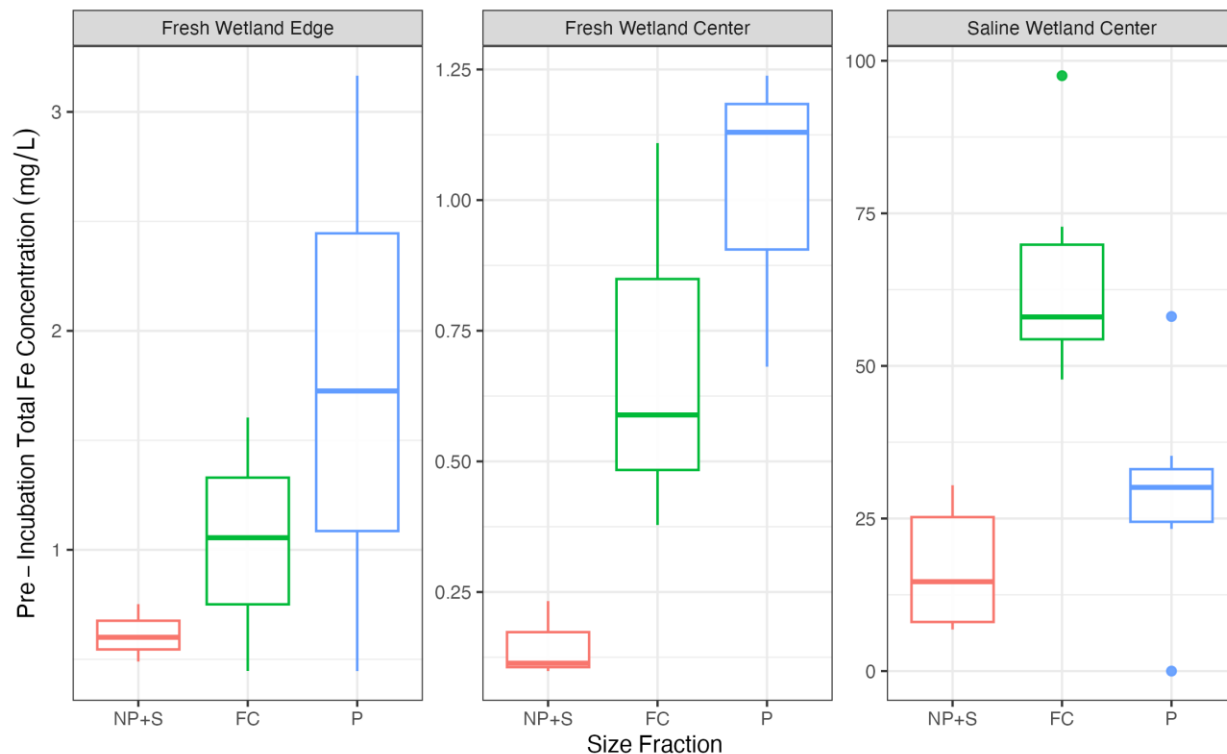
340 First, we evaluate nitrate as a potential competing terminal electron acceptor (Figure 3). The
341 highest pre-incubation dissolved ($<0.2 \mu\text{m}$) nitrate concentrations were observed in the FW-E
342 soils ($2.26 \pm 0.76 \text{ mg/L}$) compared to FW-C ($0.48 \pm 0.24 \text{ mg/L}$) and SW-C soils (0.01 ± 0.02
343 mg/L). Nitrate levels decreased significantly ($p < 0.05$) under both aerobic and anaerobic
344 conditions for the FW-E soils (Figure 3). While there was slight variability in nitrate levels in the
345 incubated FW-C and SW-C soils, none of these changes were significant ($p > 0.05$). All three
346 soils had barely detectable nitrate levels under anaerobic conditions ($0.06 - 0.19 \text{ mg/L}$)
347 suggesting that nitrate reduction likely did not prevent methanogenesis from occurring during the
348 21-day incubation.



349

350 **Figure 3.** Nitrate concentrations in samples filtered to 0.2 μm pre- and post-incubation. The
 351 instrumentation used to measure nitrate did not allow us to analyze by colloidal size fraction
 352 without compromising the instrument.

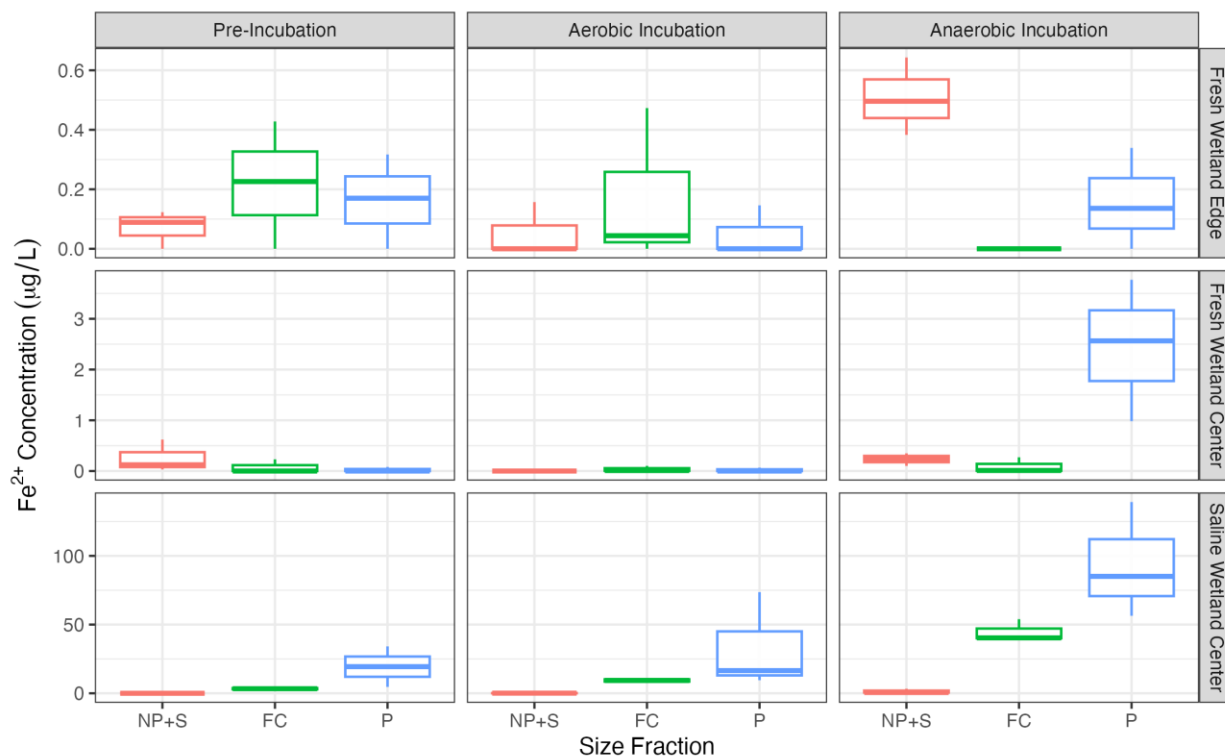
353 Iron species were measured to assess how much total iron was present initially and how much
 354 reduced iron (Fe^{2+}) was present in the aqueous phase to assess if iron reduction potentially
 355 competed with methanogenesis in any of the soil samples. Total iron at the beginning of the
 356 incubation was two orders of magnitude higher for SW-C soils compared to both freshwater soils
 357 (Figure 4; $p < 0.05$). For both freshwater soils, most of the iron was present as particulates and
 358 fine colloids with minimal nanoparticulate and soluble iron present (Figure 4). Fine colloids were
 359 the largest source of total iron for the SW-C soils and in contrast to the freshwater soils there was
 360 appreciable amounts of nanoparticulate and soluble iron prior to the incubations.



361
 362 **Figure 4.** Concentrations of total iron across size fractions prior to incubation. It was not
 363 possible to analyze post-incubation samples due to logistical constraints.

364 Similar to total iron, there was minimal Fe^{2+} present in both freshwater samples prior to the
 365 incubation (Figure 5). Adding up all three size fractions (i.e., Fe^{2+} present in all forms $< 1\mu\text{m}$),
 366 the average initial Fe^{2+} concentration was $0.38 \pm 0.25 \mu\text{g/L}$ for FW-E and $0.20 \pm 0.17 \mu\text{g/L}$ for
 367 FW-C compared to an initial concentration of $18.4 \pm 15.7 \mu\text{g/L}$ for SW-C. Particulates (i.e.,
 368 $0.45\text{-}1.0 \mu\text{m}$) were the dominant form of Fe^{2+} found in the pre-incubation samples for SW-C
 369 soils ($73 \pm 19\%$ of the Fe^{2+} pool), whereas particulates and fine colloids contributed roughly
 370 equally for the FW-E soils, and Fe^{2+} was mostly present in the smallest NP+S fraction ($67 \pm$
 371 48%) for the pre-incubation FW-C soils (Figure 5).

372 For the FW-E soils, there was a slight increase in Fe^{2+} concentrations (all fractions, $< 1\mu\text{m}$) after
 373 incubating under anaerobic and a slight decrease under aerobic conditions (Figure 5), but these
 374 changes were not significant ($p > 0.05$). When considering each size fraction independently,
 375 there was a significant increase in the NP+S fraction under anaerobic conditions and decrease
 376 under aerobic conditions ($p < 0.05$), whereas there were no significant changes in the FC or P
 377 fractions. Collectively, these results indicate that iron reduction likely did not outcompete
 378 methanogenesis during the FW-E incubations.



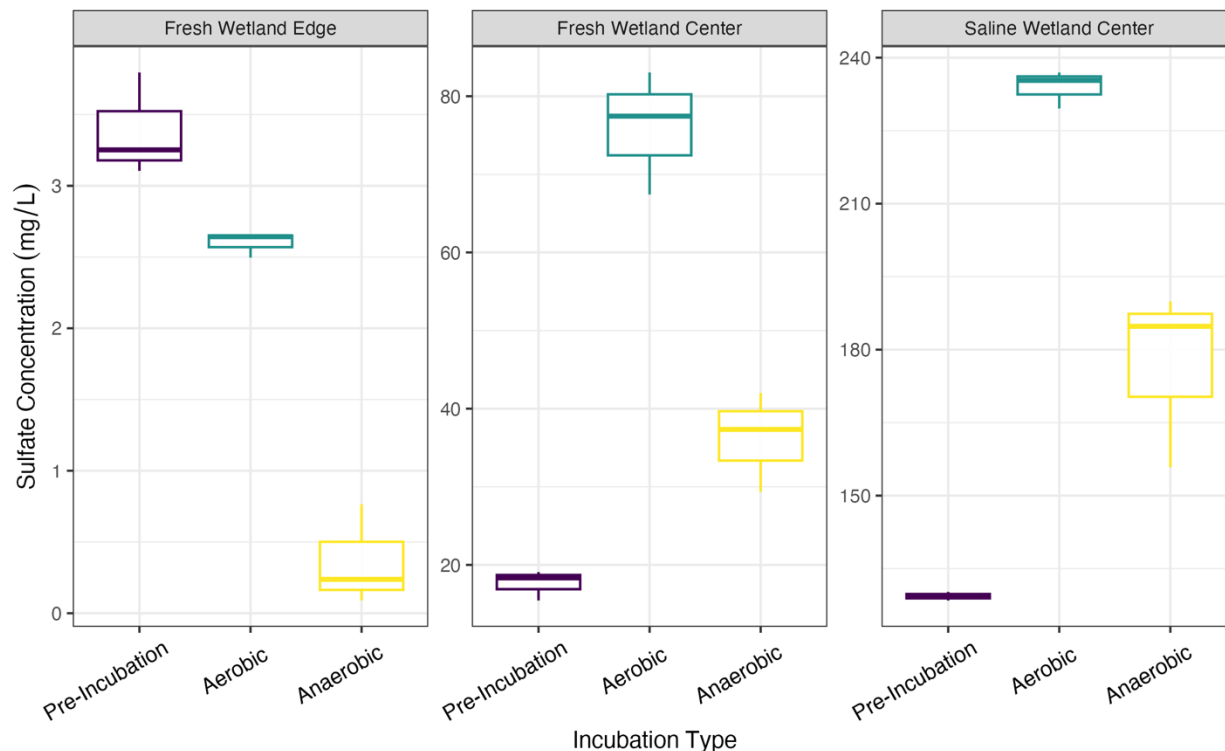
379
 380 **Figure 5.** Concentrations of Fe²⁺ across size fractions and incubation conditions. The smallest
 381 size fraction is nanoparticles plus truly soluble material (NP+S; <0.1µm), followed by fine
 382 colloids (FC; 0.1-0.45µm), then particulates (P; 0.45-1µm).

383 For the FW-C soils, Fe²⁺ concentrations (all fractions, < 1µm) similarly decreased under aerobic
 384 conditions, but the change was not significant ($p > 0.05$). In contrast to FW-E, Fe²⁺
 385 concentrations increased significantly to $2.70 \pm 1.11 \mu\text{g/L}$ (all fractions, < 1µm) under anaerobic
 386 conditions for the FW-C soils ($p < 0.05$). In the case of FW-C soils, there was a shift in the size
 387 distribution of Fe²⁺, with $84 \pm 19\%$ of the Fe²⁺ present under anaerobic conditions found in the
 388 particulate size fraction. These results suggest that iron reduction may have inhibited methane
 389 production to some extent during the 21-day incubation for FW-C soils.

390 SW-C, the soils with the lowest methane accumulation, had the highest Fe²⁺ levels initially and
 391 under both incubation conditions. In contrast to the other experiments, Fe²⁺ concentrations (all
 392 fractions, < 1µm) increased under both aerobic ($42.6 \pm 36.6 \mu\text{g/L}$) and anaerobic conditions (140
 393 $\pm 43 \mu\text{g/L}$; $p < 0.05$; Figure 5). The majority of Fe²⁺ was present as particulates under both
 394 aerobic ($69 \pm 16\%$ of the Fe²⁺ pool) and anaerobic ($65 \pm 10\%$) conditions. The fine colloid
 395 fraction contained most of the remaining Fe²⁺ with less than 1% of the Fe²⁺ present in the
 396 smallest NP+S fraction. These results suggest that iron reduction was likely an important process
 397 that limited methanogenesis for the SW-C soils.

398 Continuing down the redox ladder, dissolved (<0.2 µm) sulfate concentrations were measured to
 399 determine whether sulfate reduction may have been a factor that inhibited methanogenesis in our
 400 experiments. Average initial aqueous sulfate concentrations from the SW-C soil ($129 \pm 1 \text{ mg/L}$)
 401 were substantially higher than for the FW-E and FW-C soils ($3.38 \pm 0.36 \text{ mg/L}$ and 17.6 ± 1.9

402 mg/L, respectively; $p < 0.05$; Figure 6). During the incubations, there was a strong scent of
 403 hydrogen sulfide detected while purging the headspace of the SW-C soils held under anaerobic
 404 conditions, suggesting active sulfate reduction was occurring. Although H_2S was not directly
 405 measured, we did not smell H_2S in the other soil incubations.



406 **Figure 6.** Sulfate concentrations in samples filtered to 0.2 μm pre- and post-incubation. The
 407 instrumentation used to measure sulfate did not allow us to analyze by colloidal size fraction
 408 without compromising the instrument.
 409

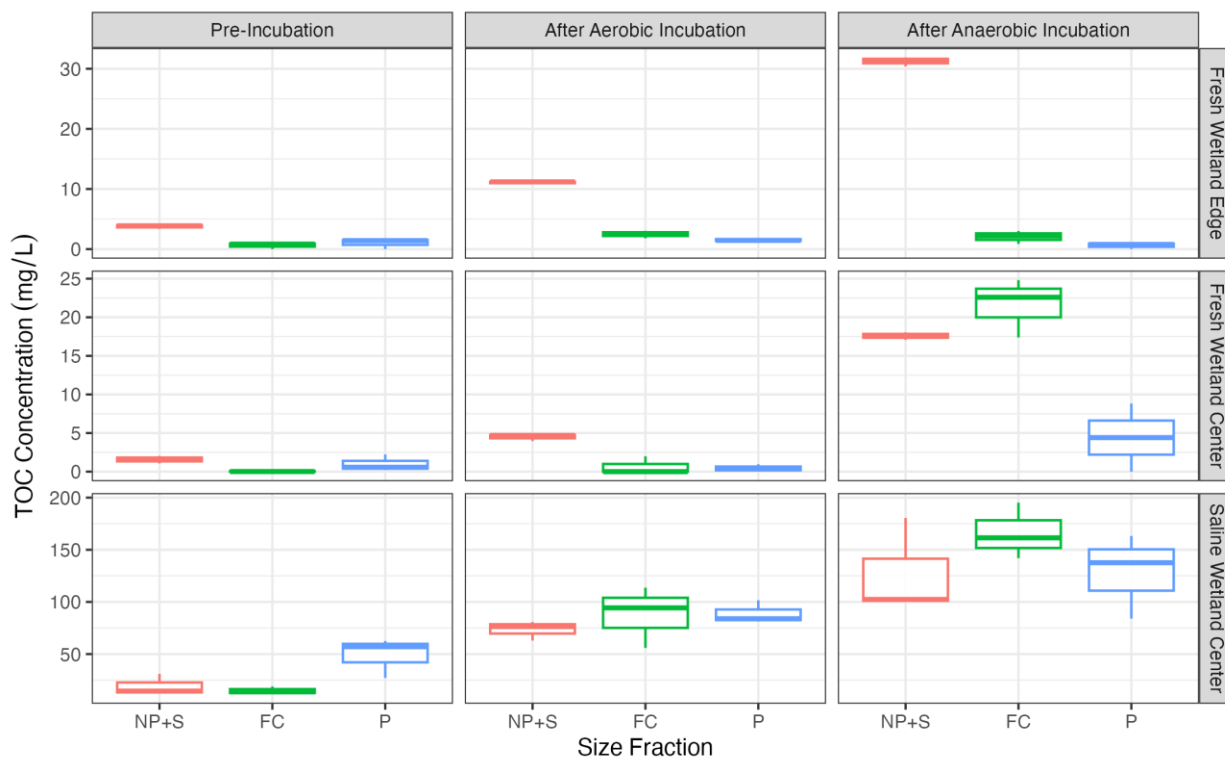
410 For the SW-C soils, sulfate levels significantly increased ($p < 0.05$) after the 21-day incubation
 411 under both aerobic (234 ± 4 mg/L) and anaerobic conditions (177 ± 18 mg/L), indicating that
 412 sulfate was not depleted as a terminal electron acceptor despite active sulfate reduction (as
 413 suggested by the H_2S scent). Interestingly, sulfate levels also increased ($p < 0.05$) for the FW-C
 414 soils under both aerobic (76.0 ± 7.9 mg/L) and anaerobic conditions (36.2 ± 6.4 mg/L), again
 415 highlighting the presence of a competing terminal electron acceptor that can inhibit
 416 methanogenesis. Though in this case we did not detect an obvious presence of H_2S . It is possible
 417 that for FW-C, iron reduction was the dominant constraint on methanogenesis.

418 Both SW-C and FW-C anaerobic incubations ended with lower sulfate concentrations than their
 419 aerobic counterparts (57.1 mg/L and 39.7 mg/L lower for SW-C and FW-C soils, respectively),
 420 suggesting a solid phase source of sulfate. Corroborating this result, we also observed a decrease
 421 in solid phase sulfur content for the SW-C and FW-C soils under both incubation conditions,
 422 except for the FW-C anaerobic incubation (Figure S4). FW-E on the other hand had lower ($p <$
 423 0.05) sulfate concentrations at the end of the incubation under aerobic (2.60 ± 0.09 mg/L) and
 424 anaerobic (0.36 ± 0.36 mg/L) conditions, suggesting that sulfur cycling did not play a major role
 425 in limiting methane production in this case.

426

3.4 Organic Carbon Content and Composition

427 The concentration, size fractionation, and composition of organic carbon was also measured to
 428 evaluate if carbon quality could potentially explain differences in GHG production across the
 429 different soil types and incubation conditions. Prior to the incubations, the TOC concentration
 430 (all size fractions combined) was significantly higher for the SW-C soils (83.0 ± 24.0 mg/L)
 431 compared to FW-E (4.97 ± 0.82 mg/L) and FW-C soils (2.59 ± 0.63 mg/L; $p < 0.05$; Figure 7)
 432 despite the FW-E solid soils having a higher percent carbon content (Figure S3). Prior to the
 433 incubations, TOC in the freshwater samples was dominated by the smallest NP+S size fraction
 434 with $64 \pm 28\%$ and $70 \pm 10\%$ of the aqueous TOC pool present as nanoparticles and soluble
 435 carbon for FW-C and FW-E, respectively (Figure 7). In contrast, only $23 \pm 9\%$ of the TOC was
 436 in the NP+S size fraction for the saline SW-C soils and most of the TOC ($58 \pm 9\%$) was in the
 437 largest particulate phase prior to incubation. Fine colloids were the smallest part of the aqueous
 438 TOC pool, representing $1 \pm 2\%$, $12 \pm 11\%$, and $19 \pm 7\%$ of TOC for FW-C, FW-E, and SW-C
 439 samples, respectively.



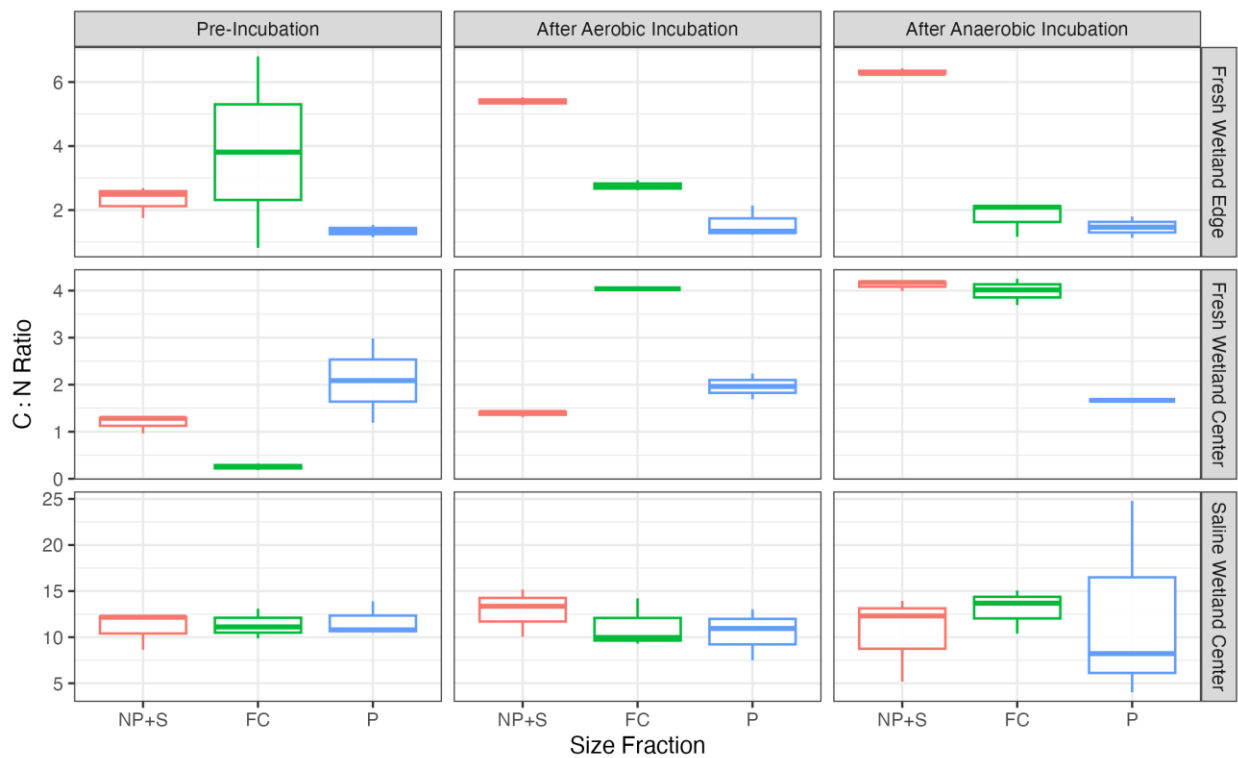
440

441 **Figure 7.** Total organic carbon across size fractions and incubation conditions. The smallest size
 442 fraction is nanoparticles plus truly soluble material (NP+S; $<0.1\mu\text{m}$), followed by fine
 443 colloids (FC; $0.1\text{-}0.45\mu\text{m}$), then particulates (P; $0.45\text{-}1\mu\text{m}$).

444 TOC concentrations increased on average for all size fractions, under both incubation conditions,
 445 and across all sites ($p < 0.05$). Across all sites, there was an average 2.8 and 1.8 times increase in
 446 particulate TOC, 12.3 and 5.9 times increase in fine colloidal TOC, and 7.2 and 3.6 times
 447 increase in nanoparticulate and soluble TOC under anaerobic and aerobic conditions,
 448 respectively. Thus, during the incubations, there was a seemingly ample and renewing supply of

449 carbon to microbial communities with a shift towards a greater proportion of FC and NP+S TOC
 450 size fractions; this increase was most evident for the freshwater and saline wetland center sites.
 451 At the end of the incubations, the fine colloidal fraction represented $44 \pm 8\%$ and $10 \pm 17\%$ of
 452 the TOC pool for FW-C, $6 \pm 3\%$ and $16 \pm 4\%$ of the TOC pool for FW-E, and $39 \pm 5\%$ and $34 \pm$
 453 6% of the TOC pool for SW-C soils under anaerobic and aerobic conditions, respectively. The
 454 nanoparticulate and soluble fraction represented $37 \pm 12\%$ and $82 \pm 11\%$ of the TOC pool for
 455 FW-C, $92 \pm 2\%$ and $73 \pm 2\%$ of the TOC pool for FW-E, and $30 \pm 12\%$ and $30 \pm 2\%$ of the TOC
 456 pool for SW-C soils under anaerobic and aerobic conditions, respectively. Finally, the SW-C soils
 457 had substantially higher TOC concentrations compared to the other two soils under both
 458 anaerobic and aerobic conditions (Figure 7; $p < 0.05$).

459 The ratio of TOC to total dissolved nitrogen (C:N ratio) was calculated to assess potential
 460 differences in organic matter composition across size fractions (Figure 8). For the saline soils,
 461 there was no significant difference in C:N ratios across all size fractions in the pre-incubated
 462 samples ($p < 0.05$). The average C:N ratios for all size fractions combined was 11.2 ± 0.5 prior to
 463 incubation, 11.2 ± 1.3 under aerobic conditions and 10.2 ± 1.0 under anaerobic conditions for
 464 SW-C soils.



465 **Figure 8.** The ratio of total organic carbon to total dissolved nitrogen (C:N) across size fractions
 466 and incubation conditions. The smallest size fraction is nanoparticulates plus truly soluble
 467 material (NP+S; $<0.1\mu\text{m}$), followed by fine colloids (FC; $0.1\text{-}0.45\mu\text{m}$), then particulates (P; 0.45-
 468 $1\mu\text{m}$).
 469

470 C:N ratios became more variable across the different size fractions under anaerobic conditions
471 with average C:N ratios of 12.3 ± 11.0 , 13.0 ± 2.4 , and 10.5 ± 4.7 for the P, FC, and NP+S size
472 fractions, respectively for SW-C soils (Figure 8), but differences between size fractions were
473 insignificant ($p > 0.05$).

474 Both freshwater soils had significantly lower C:N ratios than the saline soils, with a pre-
475 incubation average of 1.7 ± 0.2 and 2.1 ± 1.3 for FW-E and FW-C, respectively, when
476 considering all size fractions. For the FW-E soils, average C:N ratios (average of all size
477 fractions) increased significantly under both aerobic (3.8 ± 0.3) and anaerobic (5.3 ± 0.2)
478 conditions ($p < 0.05$). This change in composition was primarily driven by an increase in C:N in
479 the smallest NP+S size fraction (Figure 8), which increased to 5.4 ± 0.1 and 6.3 ± 0.1 under
480 aerobic and anaerobic conditions, respectively ($p < 0.05$). The particulate fraction remained
481 unchanged after the incubations for FW-E soils and there was a slight but insignificant decrease
482 in C:N for the fine colloid fraction ($p > 0.05$). In contrast, FW-C soils only saw an increase in
483 C:N under anaerobic conditions when considering all size fractions (3.4 ± 0.8 ; $p < 0.05$). Similar
484 to FW-E, there was an increase in C:N of the NP+S size fraction under anaerobic conditions (4.1
485 ± 0.1 ; $p < 0.05$). C:N for the fine colloid fraction also increased under both incubation conditions
486 for FW-C soils (Figure 8), but it was not possible to perform a statistical analysis due to several
487 samples having carbon and/or nitrogen concentrations of zero. In the solid soil phase, C:N ratios
488 decreased under both incubation conditions for SW-C, increased under both incubation
489 conditions for FW-C, and increased under aerobic conditions but decreased under aerobic
490 conditions for FW-E (Figure S5).

491 To further examine how carbon quality might have impacted GHG production we analyzed each
492 aqueous TOC size fraction via FT-ICR-MS and estimated the proportion of TOC present in
493 different compound classes. We did not detect significant differences between any of the size
494 fractions (Tables S1-3), so we focus our discussion on a summary of the average composition
495 across all size fractions (Table 1). The lack of variability across size fractions is likely because
496 all samples needed to be subjected to solid phase extraction to prepare samples for analysis; the
497 extraction process likely biases the results towards the composition of soluble TOC. For both
498 freshwater soils, there was a slight increase in the number of unique features (i.e., number of
499 peaks) after being incubated in aerobic conditions, but this change was not significant ($p > 0.05$).
500 In contrast there was a significant decrease in features in the saline soil under both incubation
501 conditions (Table 1; $p < 0.05$) demonstrating a loss of diversity for saline soils.

502 **Table 1.** Summary of the total number of peaks detected via FT-ICR-MS and the calculated percent contribution of different
 503 compound classes to the portion of the TOC pool captured within the analytical window. The average of all size fractions is presented
 504 here, and a breakdown by size fraction can be found in Tables S1-3.

Soil/Incubation Type	FW-E Pre- Incubation	FW-E Aerobic Incubation	FW-E Anaerobic Incubation	FW-C Pre- Incubation	FW-C Aerobic Incubation	FW-C Anaerobic Incubation	SW-C Pre- Incubation	SW-C Aerobic Incubation	SW-C Anaerobic Incubation
Compound Class									
Amino Sugars	5 ± 1	3 ± 0	2 ± 0	5 ± 1	3 ± 1	2 ± 1	4 ± 1	4 ± 1	4 ± 1
Carbohydrates	4 ± 2	2 ± 0	1 ± 1	3 ± 2	2 ± 1	1 ± 0	3 ± 1	2 ± 0	2 ± 0
Condensed Hydrocarbons	12 ± 5	18 ± 4	22 ± 3	14 ± 4	19 ± 3	22 ± 3	14 ± 6	12 ± 5	13 ± 5
Lignin	38 ± 3	50 ± 5	45 ± 1	39 ± 4	48 ± 2	45 ± 2	40 ± 4	35 ± 4	32 ± 4
Lipids	9 ± 3	4 ± 1	6 ± 2	8 ± 3	4 ± 1	6 ± 2	9 ± 5	15 ± 5	17 ± 5
Other	1 ± 0	0 ± 0	0 ± 0	1 ± 0	0 ± 0	0 ± 0	1 ± 0	0 ± 0	0 ± 0
Proteins	22 ± 5	12 ± 1	11 ± 3	21 ± 6	11 ± 2	11 ± 3	17 ± 5	21 ± 5	22 ± 4
Tannins	7 ± 3	10 ± 2	12 ± 2	8 ± 3	11 ± 2	12 ± 2	10 ± 3	8 ± 2	8 ± 2
Unsaturated Hydrocarbons	1 ± 1	1 ± 0	0 ± 0	1 ± 1	1 ± 0	1 ± 0	1 ± 1	2 ± 1	2 ± 1
Number of Peaks	9,888 ± 2,076	10,540 ± 1,673	8,773 ± 1,572	9,706 ± 2,136	10,390 ± 2,432	8,802 ± 1,513	9,688 ± 754	7,976 ± 911	7,243 ± 862

505 Lignin-like molecules were the dominant compound class for all soils both pre- and post-
506 incubation under both conditions, contributing from 29-49% of the aqueous TOC pool. The
507 proportion of lignin-like TOC in the saline soils significantly decreased under both incubation
508 conditions in contrast to an increase in the proportion of lignin-like TOC for both freshwater
509 soils under both incubation conditions (Table 1; $p < 0.05$). Protein-like molecules were the
510 second most abundant compound class, and similarly had divergent behavior between freshwater
511 and saline soils. In contrast to lignin-like molecules, the proportional abundance of protein-like
512 molecules decreased for both freshwater soils and increased in the saline soils following both
513 incubation conditions ($p < 0.05$). The third most abundant compound classes were lipid-like and
514 condensed hydrocarbon molecules. Condensed hydrocarbons increased in proportional
515 abundance following both incubation conditions in the freshwater soils ($p < 0.05$) but did not
516 change substantially in the saline soils. The relatively labile amino sugar-like TOC fraction only
517 made up ~5% of the TOC pool prior to incubation for all soils but decreased significantly for
518 both freshwater soils under both incubation conditions ($p < 0.05$) but remained unchanged in the
519 incubated saline soils ($p > 0.05$). Carbohydrate-like TOC was similarly abundant prior to
520 incubation and decreased in all soils under all incubation conditions ($p < 0.05$). Tannin-like TOC
521 followed a similar trend, decreasing for all soils under all incubation conditions ($p < 0.05$).
522 Unsaturated hydrocarbons made up a minimal fraction of the TOC pool (i.e., 0-3%) across the
523 soil types and incubation conditions (Table 1).

524 To compare molecular level data with bulk analyses, we also computed C:N ratios derived from
525 FT-ICR-MS data. Interestingly, the C:N ratios calculated with FT-ICR-MS data were
526 significantly higher ($p < 0.05$) compared to bulk C:N ratios with pre-incubation averages of 30.5
527 ± 4.0 , 32.0 ± 5.2 , and 31.9 ± 1.7 for FW-E, FW-C, and SW-C soils, respectively. FT-ICR-MS-
528 derived C:N ratios significantly decreased ($p < 0.05$) for FW-C soils under aerobic conditions
529 (28.8 ± 2.7) and increased ($p < 0.05$) for SW-C soils under both aerobic (36.4 ± 3.8) and
530 anaerobic conditions (40.0 ± 4.5), which in both cases contrasts the trends observed in bulk C:N
531 ratios. These differences between molecular level and bulk characterizations highlight the fact
532 that extracting samples and analyzing via mass spectrometry substantially narrows the analytical
533 window and range of molecules considered for calculations such as C:N ratios.

534 **4 Discussion**

535 4.1 Physiochemical Conditions of the Incubations

536 The increase in ORP after aerobic (oxidizing) incubation and a decrease in anaerobic (reducing)
537 conditions observed in both freshwater soils was expected (Figure S1). However, the counter-
538 intuitive decrease in ORP in the saline soil even under aerobic conditions may be related to the
539 association of increased ionic concentrations in saline soils with decreased oxygen solubility,
540 which leads to lower redox potentials (Herbert et al. 2015). Porewater dissolved oxygen at the
541 time of soil collection was only 2.2 mg/L at the saline site and all soils were conditioned in an
542 anaerobic chamber for 4 days prior to incubation, so the introduction of oxygen was predicted to
543 increase ORP due to the high redox potential of oxygenated water as a redox pair (Liu et al.
544 2013). Additionally, anaerobic saline soil incubations were the only ones to reach negative ORP
545 values. The increase in alkalinity and pH after anaerobic incubation of soil-water solutions is
546 also consistent with previous incubation studies (Thompson et al. 2006a, Afsar et al. 2020).

547 Increases in pH in soils subjected to anoxia have been attributed to dissolution of metal
548 oxyhydroxides and oxides (Dassonville & Renault 2002, Ponnampereuma 1972) and to
549 consumption of H⁺ in Fe-oxide reduction (Thompson et al. 2006b, Lindsay 1979). Alkalinity
550 increased to the greatest degree in saline soils in which sulfate reduction likely occurred, a
551 reaction type that yields bicarbonate (Van Breemen 1987).

552 4.2 Organic Carbon Content and Composition

553 Substantial amounts of both carbon and nitrogen were released from the soil over the course of
554 the incubations (Figures 7-8), implying that the rate of release exceeded the rate of
555 biodegradation. As in prior studies (e.g., Reddy & Patrick 1975, Yan et al. 2016, Bhattacharyya
556 et al. 2018), TOC concentrations at the end of the incubation were far greater under anaerobic
557 conditions compared to aerobic (Figure 7). Anaerobic water saturated soils tend to exhibit higher
558 concentrations of organic matter *in situ* than aerobic soils due to multiple physical, chemical, and
559 metabolic factors (Marschner 2021). Based on the differences we observed between the same
560 soils exposed to aerobic or anaerobic conditions, some potential mechanisms limiting carbon
561 biodegradation and promoting carbon accumulation in these experiments may be the low
562 energetic efficiency of anaerobic decomposition (Ponnampereuma 1972) and anoxic constraint of
563 phenol oxidase enzymes (Dunn & Freeman 2018).

564 Final concentrations of TOC in the saline soil incubates were an order of magnitude higher than
565 in freshwater soils, which is interesting given that salinity is associated with increased activity of
566 carbon-degrading enzymes (Morrissey et al. 2014) and thus could be expected to have increased
567 biodegradation. Likewise, soil extractions with seawater tend to yield lower DOC release,
568 potentially attributable in part due to flocculation of OM in response to higher ionic strength
569 (Dou et al. 2008, Kida et al. 2017). However, in the case of our incubations, the saline soils were
570 exposed to freshwater. Decreasing the ionic strength of soil-water solutions can expand the
571 diffuse double layer, causing disaggregation and destabilization of associations between OM and
572 minerals and an increase in released TOC (Kleber et al. 2021; Tomaszewski et al. 2021).

573 Iron cycling is another factor that may have influenced the amount and size of TOC released for
574 the different soils under anaerobic conditions. Mineral iron oxides bound to OM can be reduced
575 under anoxic conditions, releasing the OM formerly bound in soil (Zhao et al. 2017, Grybos et al.
576 2009). Indeed, we observed an increase in both NP+S, fine colloidal, and particulate TOC for
577 both the SW-C and FW-C soils, which had high levels of reduced Fe²⁺, whereas the FW-E soil
578 showed no evidence of iron reduction and did not release mineral-associated fine colloidal or
579 particulate TOC (Figures 5 and 7). The majority of OC of the size fractions examined was
580 present in the nanoparticulate and truly soluble fraction in freshwater soils, which follows the
581 trend seen by Afsar et al. (2020) in experiments with another freshwater wetland soil. Their
582 observation of OC in nanoparticulate size fractions being more redox-dependent than in
583 particulate size fractions also agrees with the higher increases in TOC concentrations observed
584 here in the smallest size fraction. Two exceptions to this trend were anaerobic incubations of
585 freshwater and saline wetland center soils; these soils also showed low CO₂ and methane
586 production compared to aerobic samples.

587 One other factor that may have resulted in the observed differences in TOC size fractions
588 between the freshwater and saline sites is different vegetation characteristics of the sites. The

589 saline Beaver Creek soils had a high abundance of root biomass and other plant detritus
590 associated with marsh grass (Sengupta et al., 2019), which likely contributed to the high
591 particulate TOC abundance compared to the freshwater soils. Vegetation composition at the
592 freshwater site, Old Woman Creek, on the other hand is more variable over time due to complex
593 flooding and drying regimes; depending on annual water levels, vegetation at the wetland site
594 that was sampled can vary between different macrophytes such as water lily, lotus, or cattail
595 cover (Villa et al., 2020). At the time of sampling, the freshwater wetland sites were not
596 inundated and had minimal live vegetation present.

597 4.3 Greenhouse Gas Production and Competing Redox Reactions

598 The low methane production in both fresh and saline wetland center soils can be attributed to the
599 reduction of species (e.g., NO_3^- , MnO_2 , Fe^{3+} , SO_4^{2-}) higher on the redox ladder outcompeting
600 methanogenesis. Nitrate was depleted for all soil types under anaerobic conditions. Iron reduction
601 was prominent for both wetland center soils as shown by Fe^{2+} concentrations (Figure 5) and was
602 likely an important reaction competing with methanogenesis similar to findings from other
603 experimental studies (e.g., Helton et al. 2019). Interestingly, the FW-E soils, which produced 47
604 times more methane under anaerobic conditions than the FW-C soils (Figure 2), had higher pre-
605 incubation concentrations of total iron than the FW-C soil (Figure 4). However, FW-E did not
606 produce appreciable amounts of Fe^{2+} , suggesting that significant iron reduction did not occur in
607 the wetland edge soil and/or there was not a prominent solid phase iron source. A variety of
608 factors are known to influence the availability of Fe^{3+} in soils, including acidic pH and low ORP
609 (Colombo et al. 2014). The freshwater wetland center soil, which appeared to host iron
610 reduction, had lower pH values during anaerobic incubations than the wetland edge soil, though
611 not as acidic as conditions typically associated with high iron solubility (Borch 2010). Low
612 redox potential is also associated with iron reduction, and the FW-E soil, which had no increase
613 in Fe^{2+} , did have higher redox potentials than the other soils. Methane production took about four
614 days to initiate in the FW-E soils, perhaps as a result of competing redox reactions that exhausted
615 all available terminal electron acceptors (Figure 2). This difference in iron cycling between the
616 two freshwater sites perhaps related to the fact that FW-C soils are more frequently flooded and
617 anoxic compared to FW-E, which is only periodically inundated (USDA Natural Resources
618 Conservation Service n.d).

619 Sulfate reduction was another important competing redox reaction in the saline soil under
620 anaerobic conditions. Although we cannot discount sulfate reduction as a competing reaction
621 with methanogenesis for the freshwater wetland center soil, which had high levels of sulfate
622 (Figure 6), the odor of H_2S emerging from the saline samples is clear evidence that sulfate
623 reduction was active for the saline soils. Solid phase sulfur content was relatively high in the
624 saline soil prior to incubations, and decreased markedly under both incubation conditions (Figure
625 S4). Potential sources of sulfate might include oxidation of iron and sulfur containing minerals
626 under aerobic conditions or reductive dissolution of minerals under anaerobic conditions (Van
627 Breemen 1988). It is unclear how long the soils would need to be incubated (or flooded in the
628 case of the natural ecosystem setting) to exhaust the large source of mineral sulfur and initiate
629 methanogenesis, particularly for the saline soil.

630 Experimental results from this study highlight the importance in considering the diversity of size
631 fractions present in soil-water matrices for interpreting drivers of GHG production. For example,

632 results from the anaerobic incubation showed that iron reduction played a direct role in limiting
633 methane production. However, measuring dissolved iron via filtration would have masked this
634 finding. The majority of Fe^{2+} in soils with high concentrations was measured in the largest
635 particulate size fraction (0.45 – 1 μm). Colloids greater than 0.45 μm are often excluded from
636 studies of OM characterization and/or GHG production, but in this study the larger size fraction
637 was key in providing evidence for iron reduction as a competing redox reaction and potential
638 mechanism for mineral-associated TOC release.

639 Considering colloidal and particulate size fractions of TOC also yielded insight into the
640 mechanisms underlying different responses in aerobic CO_2 production across the different soil
641 types. Aerobic CO_2 production was highest for both freshwater soils, which had a much higher
642 proportion of pre-incubation OM in the NP+S fraction ($64 \pm 28\%$ and $70 \pm 10\%$ for FW-C and
643 FW-E, respectively) compared to the SW-C soil ($24 \pm 9\%$). This finding contrasts conceptual
644 models for OM bioavailability in aquatic settings. For example, larger colloidal and particulate
645 OM is thought to be more bioavailable in marine surface waters (Benner and Amon, 2015), but
646 active association or disassociation with mineral surfaces may complicate this model in
647 terrestrial systems (Yan et al. 2018).

648 TOC quantity was clearly not the primary driver of aerobic respiration in our experiments
649 considering the low CO_2 production for SW-C soils (Figure 1), which had an order of magnitude
650 higher TOC content (Figure 7). Rather, carbon quality was likely a key constraint on aerobic
651 respiration. The freshwater soils not only had a higher proportion of truly soluble and
652 nanoparticulate TOC that remained unassociated with minerals, they also had a substantially
653 higher amount of nitrogen relative to carbon compared to the SW-C soils. The very low C:N
654 ratios in the freshwater soils (1.7 ± 0.2 and 1.4 ± 0.3 for FW-E and FW-C, respectively) are
655 reflective of microbial detritus, whereas the C:N ratios for SW-C of 11.2 ± 0.5 are more
656 reflective of vegetation detritus (Bianchi et al. 2007). This microbially-derived OM appeared to
657 be much more readily bioavailable compared to the OM present in the SW-C soils, which is
658 consistent with observations that low C:N ratios in soils is often highly bioavailable (Liu et al.
659 2016). These differences in OM composition would not have been as evident without examining
660 the elemental composition of different size fractions. Our characterization of OM composition
661 via FT-ICR-MS, alone, would have suggested a more homogenous composition across soils and
662 incubations (Table 1) due to the smaller analytical window this method provides (Qi et al. 2022).

663 **5 Conclusions**

664 Coastal wetlands contain dynamic carbon pools that are anticipated to face increased stressors in
665 the form of SLR and increased occurrence and severity of extreme weather events (Ward et al.
666 2020, LaFond-Hudson and Sulman, 2023). These changes are expected to alter coastal wetland
667 redox conditions (Regier et al. 2023) and organic matter cycling (Smith et al. 2023). In this
668 study, we experimentally probed several major gaps in our understanding of the properties and
669 processes that mediate 1) GHG emissions from coastal wetlands and 2) the mobility of carbon in
670 coastal wetland soils across a more complete size class spectrum than is typically studied.

671 First, we quantified how the presence of a variety of terminal electron acceptors (i.e., nitrate,
672 iron, and sulfate) associated with distinct soil types and inundation history inhibit methane
673 production under anaerobic conditions. By characterizing a spectrum of different size fractions

674 (e.g., soluble, nanoparticulates, fine colloids, and particulates), we were able to develop
675 mechanistic insight into why and under what conditions certain redox reactions can limit
676 methanogenesis. We found that reduction of mineral-phase iron into particulate and colloidal
677 Fe^{2+} was one major factor limiting methanogenesis in both fresh and saline wetland center soils
678 along with sulfate reduction in the saline soil.

679 We used the same size fractionation technique to characterize the aqueous organic matter pool to
680 mechanistically understand why aerobic CO_2 production varied substantially across the three
681 different studied soils. We found that soils with a higher proportion of soluble molecules had
682 substantially higher rates of aerobic respiration compared to soils with a higher proportion of
683 colloidal and particulate carbon. Likewise, we found that carbon quality was more important
684 than carbon quantity in driving high respiration rates. Finally, we found that colloidal organic
685 matter could be a prominent, and overlooked, component of the pool of carbon that is mobile in
686 wetland soil environments, particularly for the saline soils we investigated. The high proportion
687 of colloidal OM found in the saline wetland soil, OM that typically goes uncharacterized, may be
688 a major component of the carbon that is laterally transported from coastal wetlands to the ocean.

689 **Acknowledgments**

690 This research was performed on project award 60097 from the Environmental Molecular
691 Sciences Laboratory, a DOE Office of Science User Facility sponsored by the Biological and
692 Environmental Research program under Contract No. DE-AC05-76RL01830. The samples used
693 for this study were collected at field sites stewarded by COMPASS-FME, a multi-institutional
694 project supported by DOE-BER as part of the Environmental System Science Program. We
695 thank the University of Toledo field team for support maintaining the research sites and Kaizad
696 Patel for helping with soil sample collection at Old Woman Creek. We thank Don Lentz, the
697 Hancock Timber Company, and Washington Department of Fish & Wildlife for access to the
698 Beaver Creek field site. We thank the NOAA-NERR program for access to the Old Woman
699 Creek site and producing the datasets used for site context. Data were collected via the NERR
700 System-wide Monitoring Program (<https://cdmo.baruch.sc.edu/>) for Old Woman Creek. We
701 thank Kathleen Munson and Nubia Nieto Pereira for assistance with ICP-OES analyses as well
702 as Opal Otenburg and Allison Myers-Pigg for ion chromatograph analyses.

703

704 **Open Research**

705 All data used in this study are available at the Figshare.com repository via
706 <https://doi.org/10.6084/m9.figshare.c.6827016.v3> with a publicly available CC BY 4.0 license.
707 To elevate findability by the biogeosciences community, the final dataset will be cross-
708 referenced on the Environmental System Science Data Infrastructure for a Virtual Ecosystem
709 (ESS-DIVE) data repository upon acceptance of the manuscript.

710

711 **References**

712 Afsar, M. Z., Goodwin, C., Beebe Jr, T. P., Jaisi, D. P., & Jin, Y. (2020). Quantification and
713 molecular characterization of organo-mineral associations as influenced by redox
714 oscillations. *Science of the Total Environment*, 704, 135454.

- 715 Afsar, M.Z., Vasilas, B. & Jin, Y. (2023). Organo-mineral associations and size-fractionated
716 colloidal organic carbon dynamics in a redox-controlled wetland. *Geoderma*, 439, 116667.
- 717 Altor, A. E., & Mitsch, W. J. (2008). Pulsing hydrology, methane emissions and carbon dioxide
718 fluxes in created marshes: A 2-year ecosystem study. *Wetlands*, 28(2), 423-438.
- 719 Bailey, V. L., Smith, A. P., Tfaily, M., Fansler, S. J., & Bond-Lamberty, B. (2017). Differences
720 in soluble organic carbon chemistry in pore waters sampled from different pore size
721 domains. *Soil Biology and Biochemistry*, 107, 133-143.
- 722 Benner, R., & Amon, R. M. (2015). The size-reactivity continuum of major bioelements in the
723 ocean. *Annual review of marine science*, 7, 185-205.
- 724 Bhattacharyya, A., Campbell, A. N., Tfaily, M. M., Lin, Y., Kukkadapu, R. K., Silver, W. L., ...
725 & Pett-Ridge, J. (2018). Redox fluctuations control the coupled cycling of iron and carbon
726 in tropical forest soils. *Environmental science & technology*, 52(24), 14129-14139.
- 727 Bianchi, T. S., Wysocki, L. A., Stewart, M., Filley, T. R., & McKee, B. A. (2007). Temporal
728 variability in terrestrially-derived sources of particulate organic carbon in the lower
729 Mississippi River and its upper tributaries. *Geochimica et Cosmochimica Acta*, 71(18),
730 4425-4437.
- 731 Borch, T., Kretzschmar, R., Kappler, A., Cappellen, P. V., Ginder-Vogel, M., Voegelin, A., &
732 Campbell, K. (2010). Biogeochemical redox processes and their impact on contaminant
733 dynamics. *Environmental science & technology*, 44(1), 15-23.
- 734 Buettner, S. W., Kramer, M. G., Chadwick, O. A., & Thompson, A. (2014). Mobilization of
735 colloidal carbon during iron reduction in basaltic soils. *Geoderma*, 221, 139-145.
- 736 Chen, C., Hall, S. J., Coward, E., & Thompson, A. (2020). Iron-mediated organic matter
737 decomposition in humid soils can counteract protection. *Nature communications*, 11(1), 1-
738 13.
- 739 Chu, S. N., Wang, Z. A., Gonneea, M. E., Kroeger, K. D., & Ganju, N. K. (2018). Deciphering
740 the dynamics of inorganic carbon export from intertidal salt marshes using high-frequency
741 measurements. *Marine Chemistry*, 206, 7-18.
- 742 Clark, J. M., Lane, S. N., Chapman, P. J., & Adamson, J. K. (2007). Export of dissolved organic
743 carbon from an upland peatland during storm events: Implications for flux estimates.
744 *Journal of Hydrology*, 347(3-4), 438-447.
- 745 Colombo, C., Palumbo, G., He, J. Z., Pinton, R., & Cesco, S. (2014). Review on iron availability
746 in soil: interaction of Fe minerals, plants, and microbes. *Journal of soils and sediments*,
747 14(3), 538-548.
- 748 Dassonville, F., & Renault, P. (2002). Interactions between microbial processes and geochemical
749 transformations under anaerobic conditions: a review. *Agronomie*, 22(1), 51-68.
- 750 Dittmar, T., Koch, B., Hertkorn, N., & Kattner, G. (2008). A simple and efficient method for
751 The Solid-phase extraction of dissolved organic matter (SPE-DOM) from seawater.
752 *Limnology and Oceanography: Methods*, 6(6), 230-235. doi:10.4319/lom.2008.6.230
- 753 Dou, F., Ping, C. L., Guo, L., & Jorgenson, T. (2008). Estimating the impact of seawater on the
754 production of soil water-extractable organic carbon during coastal erosion. *Journal of*
755 *environmental quality*, 37(6), 2368-2374.
- 756 Dunn, C., & Freeman, C. (2018). The role of molecular weight in the enzyme-inhibiting effect of
757 phenolics: the significance in peatland carbon sequestration. *Ecological Engineering*, 114,
758 162-166.

- 759 Feng, J., & Hsieh, Y. P. (1998). Sulfate reduction in freshwater wetland soils and the effects of
760 sulfate and substrate loading (Vol. 27, No. 4, pp. 968-972). American Society of
761 Agronomy, Crop Science Society of America, and Soil Science Society of America.
- 762 Freeman, C., Ostle, N., & Kang, H. (2001). An enzymic 'latch' on a global carbon store. *Nature*,
763 409(6817), 149-149.
- 764 Grybos, M., Davranche, M., Gruau, G., Petitjean, P., & Pédrot, M. (2009). Increasing pH drives
765 organic matter solubilization from wetland soils under reducing conditions. *Geoderma*,
766 154(1-2), 13-19.
- 767 Helton, A. M., Ardón, M., & Bernhardt, E. S. (2019). Hydrologic context alters greenhouse gas
768 feedbacks of coastal wetland salinization. *Ecosystems*, 22(5), 1108-1125.
- 769 Herbert, E. R., Boon, P., Burgin, A. J., Neubauer, S. C., Franklin, R. B., Ardón, M., ... & Gell, P.
770 (2015). A global perspective on wetland salinization: ecological consequences of a
771 growing threat to freshwater wetlands. *Ecosphere*, 6(10), 1-43.
- 772 Ho, D. T., Ferrón, S., Engel, V. C., Anderson, W. T., Swart, P. K., Price, R. M., & Barbero, L.
773 (2017). Dissolved carbon biogeochemistry and export in mangrove-dominated rivers of
774 the Florida Everglades. *Biogeosciences*, 14(9), 2543-2559.
- 775 Kida, M., Tomotsune, M., Iimura, Y., Kinjo, K., Ohtsuka, T., & Fujitake, N. (2017). High
776 salinity leads to accumulation of soil organic carbon in mangrove soil. *Chemosphere*, 177,
777 51-55.
- 778 Kim, H. S., & Pfaender, F. K. (2005). Effects of microbially mediated redox conditions on
779 PAH– soil interactions. *Environmental science & technology*, 39(23), 9189-9196.
- 780 Kleber, M., Bourg, I. C., Coward, E. K., Hansel, C. M., Myneni, S. C., & Nunan, N. (2021).
781 Dynamic interactions at the mineral–organic matter interface. *Nature Reviews Earth &
782 Environment*, 2(6), 402-421.
- 783 Lal, R., Monger, C., Nave, L., & Smith, P. (2021). The role of soil in regulation of climate.
784 *Philosophical Transactions of the Royal Society B*, 376(1834), 20210084.
- 785 LaFond-Hudson, S., & Sulman, B. (2023). Modeling strategies and data needs for representing
786 coastal wetland vegetation in land surface models. *New Phytologist*, 238(3), 938-951.
- 787 Lindsay, W. L. (1979). *Chemical equilibria in soils*. John Wiley and Sons Ltd..
- 788 Liu, C. G., Xue, C., Lin, Y. H., & Bai, F. W. (2013). Redox potential control and applications in
789 microaerobic and anaerobic fermentations. *Biotechnology advances*, 31(2), 257-265.
- 790 Liu, M., Ussiri, D. A., & Lal, R. (2016). Soil organic carbon and nitrogen fractions under
791 different land uses and tillage practices. *Communications in Soil Science and Plant
792 Analysis*, 47(12), 1528-1541.
- 793 Lønborg, C., Carreira, C., Jickells, T., & Álvarez-Salgado, X. A. (2020). Impacts of global
794 change on ocean dissolved organic carbon (DOC) cycling. *Frontiers in Marine Science*, 7,
795 466.
- 796 Magen, C., Lapham, L. L., Pohlman, J. W., Marshall, K., Bosman, S., Casso, M., & Chanton, J.
797 P. (2014). A simple headspace equilibration method for measuring dissolved methane.
798 *Limnology and Oceanography: Methods*, 12(9), 637-650.
- 799 Maher, D.T., Santos, I.R., Golsby-Smith, L., Gleeson, J. and Eyre, B.D., 2013. Groundwater-
800 derived dissolved inorganic and organic carbon exports from a mangrove tidal creek: The
801 missing mangrove carbon sink?. *Limnology and Oceanography*, 58(2), pp.475-488.
- 802 Marín-Spiotta, E., Gruley, K. E., Crawford, J., Atkinson, E. E., Miesel, J. R., Greene, S., ... &
803 Spencer, R. G. M. (2014). Paradigm shifts in soil organic matter research affect

- 804 interpretations of aquatic carbon cycling: transcending disciplinary and ecosystem
805 boundaries. *Biogeochemistry*, 117(2), 279-297.
- 806 Marschner, P. (2021). Processes in submerged soils—linking redox potential, soil organic matter
807 turnover and plants to nutrient cycling. *Plant and Soil*, 464(1), 1-12.
- 808 Moomaw, W. R., Chmura, G. L., Davies, G. T., Finlayson, C. M., Middleton, B. A., Natali, S.
809 M., ... & Sutton-Grier, A. E. (2018). Wetlands in a changing climate: science, policy and
810 management. *Wetlands*, 38(2), 183-205.
- 811 Morrissey, E. M., Gillespie, J. L., Morina, J. C., & Franklin, R. B. (2014). Salinity affects
812 microbial activity and soil organic matter content in tidal wetlands. *Global change
813 biology*, 20(4), 1351-1362.
- 814 Neubauer, S. C., Franklin, R. B., & Berrier, D. J. (2013). Saltwater intrusion into tidal freshwater
815 marshes alters the biogeochemical processing of organic carbon. *Biogeosciences*, 10(12),
816 8171-8183.
- 817 NOAA National Estuarine Research Reserve System (NERRS). System-wide Monitoring
818 Program. Data accessed from the NOAA NERRS Centralized Data Management Office
819 website: <http://www.nerrsdata.org>; accessed 5 October 2022.
- 820 Noe, G. B., Krauss, K. W., Lockaby, B. G., Conner, W. H., & Hupp, C. R. (2013). The effect of
821 increasing salinity and forest mortality on soil nitrogen and phosphorus mineralization in
822 tidal freshwater forested wetlands. *Biogeochemistry*, 114(1), 225-244.
- 823 Olsson, L., Ye, S., Yu, X., Wei, M., Krauss, K. W., & Brix, H. (2015). Factors influencing CO₂
824 and CH₄ emissions from coastal wetlands in the Liaohe Delta, Northeast China.
825 *Biogeosciences*, 12(16), 4965-4977.
- 826 Orton, D.J., Tfaily, M.M., Moore, R.J., LaMarche, B.L., Zheng, X., Fillmore, T.L., Chu, R.K.,
827 Weitz, K.K., Monroe, M.E., Kelly, R.T. and Smith, R.D. (2018). A customizable flow
828 injection system for automated, high throughput, and time sensitive ion mobility
829 spectrometry and mass spectrometry measurements. *Analytical chemistry*, 90(1), pp.737-
830 744.
- 831 Parkin, T. B. (1987). Soil microsites as a source of denitrification variability. *Soil Science
832 Society of America Journal*, 51(5), 1194-1199.
- 833 Patel, K. F., Bond-Lamberty, B., Jian, J., Morris, K. A., McKeever, S. A., Norris, C. G., ... &
834 Bailey, V. L. (2022). Carbon flux estimates are sensitive to data source: a comparison of
835 field and lab temperature sensitivity data. *Environmental Research Letters*, 17(11),
836 113003.
- 837 Poffenbarger, H. J., Needelman, B. A., & Megonigal, J. P. (2011). Salinity influence on methane
838 emissions from tidal marshes. *Wetlands*, 31(5), 831-842.
- 839 Ponnamperna, F. N. (1972). The chemistry of submerged soils. *Advances in agronomy*, 24, 29-
840 96.
- 841 Qi, Y., Xie, Q., Wang, J. J., He, D., Bao, H., Fu, Q. L., ... & Fu, P. (2022). Deciphering dissolved
842 organic matter by Fourier transform ion cyclotron resonance mass spectrometry (FT-ICR
843 MS): from bulk to fractions and individuals. *Carbon Research*, 1(1), 3.
- 844 Qu, W., Li, J., Han, G., Wu, H., Song, W., & Zhang, X. (2019). Effect of salinity on the
845 decomposition of soil organic carbon in a tidal wetland. *Journal of Soils and Sediments*,
846 19(2), 609-617.
- 847 R Core Team. (2021). R: A language and environment for statistical computing. R Foundation
848 for Statistical Computing, Vienna, Austria.

- 849 Reddy, K. R., & Patrick Jr, W. H. (1975). Effect of alternate aerobic and anaerobic conditions on
850 redox potential, organic matter decomposition and nitrogen loss in a flooded soil. *Soil*
851 *Biology and Biochemistry*, 7(2), 87-94.
- 852 Regier, P., Ward, N. D., Indivero, J., Wiese Moore, C., Norwood, M., & Myers-Pigg, A. (2021).
853 Biogeochemical control points of connectivity between a tidal creek and its floodplain.
854 *Limnology and Oceanography Letters*, 6(3), 134-142.
- 855 Regier, P. J., Ward, N. D., Myers-Pigg, A. N., Grate, J., Freeman, M. J., & Ghosh, R. N. (2023).
856 Seasonal drivers of dissolved oxygen across a tidal creek-marsh interface revealed by
857 machine learning. *Limnology and Oceanography*.
- 858 Rod, K. A., Patel, K. F., Kumar, S., Cantando, E., Leng, W., Kukkadapu, R. K., ... & Kemner, K.
859 M. (2020). Dispersible Colloid Facilitated Release of Organic Carbon From Two
860 Contrasting Riparian Sediments. *Frontiers in Water*, 2, 67.
- 861 Rodrigo-Comino, J., López-Vicente, M., Kumar, V., Rodríguez-Seijo, A., Valkó, O., Rojas, C.,
862 ... & Panagos, P. (2020). Soil science challenges in a new era: a transdisciplinary overview
863 of relevant topics. *Air, Soil and Water Research*, 13, 1178622120977491.
- 864 Santos, I. R., Burdige, D. J., Jennerjahn, T. C., Bouillon, S., Cabral, A., Serrano, O., ... &
865 Tamborski, J. J. (2021). The renaissance of Odum's outwelling hypothesis in Blue
866 Carbon'science. *Estuarine, Coastal and Shelf Science*, 255, 107361.
- 867 Schmidt, M. W., Torn, M. S., Abiven, S., Dittmar, T., Guggenberger, G., Janssens, I. A., ... &
868 Trumbore, S. E. (2011). Persistence of soil organic matter as an ecosystem property.
869 *Nature*, 478(7367), 49-56.
- 870 Sengupta, A., Indivero, J., Gunn, C., Tfaily, M.M., Chu, R.K., Toyoda, J., Bailey, V.L., Ward,
871 N.D. and Stegen, J.C. (2019). Spatial gradients in soil-carbon character of a coastal
872 forested floodplain are associated with abiotic features, but not microbial communities.
873 *Biogeosciences*, 16, 3911-3928.
- 874 Sengupta, A., Stegen, J.C., Bond-Lamberty, B., Rivas-Ubach, A., Zheng, J., Handakumbura,
875 P.P., Norris, C., Peterson, M.J., Yabusaki, S.B., Bailey, V.L. and Ward, N.D. (2021).
876 Antecedent conditions determine the biogeochemical response of coastal soils to seawater
877 exposure. *Soil Biology and Biochemistry*, 153, 108104.
- 878 Sjögersten, S., Black, C. R., Evers, S., Hoyos-Santillan, J., Wright, E. L., & Turner, B. L. (2014).
879 Tropical wetlands: a missing link in the global carbon cycle?. *Global biogeochemical*
880 *cycles*, 28(12), 1371-1386.
- 881 Smith, A. J., McGlathery, K., Chen, Y., Ewers Lewis, C. J., Doney, S. C., Gedan, K., ... &
882 Kirwan, M. L. (2023). Compensatory Mechanisms Absorb Regional Carbon Losses
883 Within a Rapidly Shifting Coastal Mosaic. *Ecosystems*, 1-15.
- 884 Spivak, A. C., Sanderman, J., Bowen, J. L., Canuel, E. A., & Hopkinson, C. S. (2019). Global-
885 change controls on soil-carbon accumulation and loss in coastal vegetated ecosystems.
886 *Nature Geoscience*, 12(9), 685-692.
- 887 Stagg, C. L., Baustian, M. M., Perry, C. L., Carruthers, T. J., & Hall, C. T. (2018). Direct and
888 indirect controls on organic matter decomposition in four coastal wetland communities
889 along a landscape salinity gradient. *Journal of Ecology*, 106(2), 655-670.
- 890 Stagg, C. L., Schoolmaster, D. R., Krauss, K. W., Cormier, N., & Conner, W. H. (2017). Causal
891 mechanisms of soil organic matter decomposition: deconstructing salinity and flooding
892 impacts in coastal wetlands. *Ecology*, 98(8), 2003-2018.

- 893 Stockmann, U., Adams, M. A., Crawford, J. W., Field, D. J., Henakaarchchi, N., Jenkins, M., ...
894 & Zimmermann, M. (2013). The knowns, known unknowns and unknowns of
895 sequestration of soil organic carbon. *Agriculture, Ecosystems & Environment*, 164, 80-99.
- 896 Stookey, L. L. (1970). Ferrozine---a new spectrophotometric reagent for iron. *Analytical*
897 *chemistry*, 42(7), 779-781.
- 898 Thompson, A., Chadwick, O. A., Boman, S., & Chorover, J. (2006a). Colloid mobilization
899 during soil iron redox oscillations. *Environmental science & technology*, 40(18), 5743-
900 5749.
- 901 Thompson, A., Chadwick, O. A., Rancourt, D. G., & Chorover, J. (2006b). Iron-oxide
902 crystallinity increases during soil redox oscillations. *Geochimica et Cosmochimica Acta*,
903 70(7), 1710-1727.
- 904 Tolić, N., Liu, Y., Liyu, A., Shen, Y., Tfaily, M.M., Kujawinski, E.B., Longnecker, K., Kuo,
905 L.J., Robinson, E.W., Paša-Tolić, L. and Hess, N.J. (2017). Formularity: software for
906 automated formula assignment of natural and other organic matter from ultrahigh-
907 resolution mass spectra. *Analytical chemistry*, 89(23), pp.12659-12665.
- 908 Tomaszewski, E. J., Coward, E. K., & Sparks, D. L. (2021). Ionic strength and species drive
909 iron-carbon adsorption dynamics: implications for carbon cycling in future coastal
910 environments. *Environmental Science & Technology Letters*, 8(8), 719-724.
- 911 Tully, K., Gedan, K., Epanchin-Niell, R., Strong, A., Bernhardt, E. S., BenDor, T., ... & Weston,
912 N. B. (2019). The invisible flood: The chemistry, ecology, and social implications of
913 coastal saltwater intrusion. *BioScience*, 69(5), 368-378.
- 914 USDA Natural Resources Conservation Service. (n.d.). Web soil survey. Retrieved November 7,
915 2019 for Beaver Creek and November 22, 2023 for Old Woman Creek, from
916 <https://websoilsurvey.nrcs.usda.gov/app/WebSoilSurvey.aspx>
- 917 Van Breemen, N. (1987). Effects of redox processes on soil acidity. *Netherlands Journal of*
918 *Agricultural Science*, 35(3), 271-279.
- 919 Van Breemen, N. (1988). Redox processes of iron and sulfur involved in the formation of acid
920 sulfate soils. In *Iron in soils and clay minerals* (pp. 825-841). Dordrecht: Springer
921 Netherlands.
- 922 Villa, J. A., & Bernal, B. (2018). Carbon sequestration in wetlands, from science to practice: An
923 overview of the biogeochemical process, measurement methods, and policy framework.
924 *Ecological Engineering*, 114, 115-128.
- 925 Villa, J. A., Ju, Y., Stephen, T., Rey-Sanchez, C., Wrighton, K. C., & Bohrer, G. (2020). Plant-
926 mediated methane transport in emergent and floating-leaved species of a temperate
927 freshwater mineral-soil wetland. *Limnology and Oceanography*, 65(7), 1635-1650.
- 928 Wang, F., Lu, X., Sanders, C. J., & Tang, J. (2019). Tidal wetland resilience to sea level rise
929 increases their carbon sequestration capacity in United States. *Nature communications*,
930 10(1), 1-11.
- 931 Wang, Y., Wang, H., He, J. S., & Feng, X. (2017). Iron-mediated soil carbon response to water-
932 table decline in an alpine wetland. *Nature communications*, 8(1), 1-9.
- 933 Wanninkhof, R. (2014). Relationship between wind speed and gas exchange over the ocean
934 revisited. *Limnology and Oceanography: Methods*, 12(6), 351-362.
- 935 Ward, N. D., Megonigal, J. P., Bond-Lamberty, B., Bailey, V. L., Butman, D., Canuel, E. A., ...
936 & Windham-Myers, L. (2020). Representing the function and sensitivity of coastal
937 interfaces in Earth system models. *Nature Communications*, 11(1), 1-14.

- 938 Wiesenburg, D. A., & Guinasso Jr, N. L. (1979). Equilibrium solubilities of methane, carbon
939 monoxide, and hydrogen in water and sea water. *Journal of chemical and engineering*
940 *data*, 24(4), 356-360.
- 941 Weiss, R. F., & Price, B. A. (1980). Nitrous oxide solubility in water and seawater. *Marine*
942 *chemistry*, 8(4), 347-359.
- 943 Weston, N. B., Vile, M. A., Neubauer, S. C., & Velinsky, D. J. (2011). Accelerated microbial
944 organic matter mineralization following salt-water intrusion into tidal freshwater marsh
945 soils. *Biogeochemistry*, 102(1), 135-151.
- 946 Wuebbles, D., Cardinale, B., Cherkauer, K., Davidson-Arnott, R., Hellmann, J., Infante, D. and
947 Ballinger, A. (2019). An assessment of the impacts of climate change on the Great
948 Lakes. *Environmental Law & Policy Center*, 760.
- 949 Yabusaki, S. B., Myers-Pigg, A. N., Ward, N. D., Waichler, S. R., Sengupta, A., Hou, Z., ... &
950 Gunn, C. M. (2020). Floodplain inundation and salinization from a recently restored first-
951 order tidal stream. *Water Resources Research*, 56(7), e2019WR026850.
- 952 Yan, J., Lazouskaya, V., & Jin, Y. (2016). Soil colloid release affected by dissolved organic
953 matter and redox conditions. *Vadose Zone Journal*, 15(3).
- 954 Yan, J., Manelski, R., Vasilas, B., & Jin, Y. (2018). Mobile colloidal organic carbon: an
955 underestimated carbon pool in global carbon cycles?. *Frontiers in Environmental Science*,
956 6, 148.
- 957 Yu, C., Xie, S., Song, Z., Xia, S., & Åström, M. E. (2021). Biogeochemical cycling of iron
958 (hydr-) oxides and its impact on organic carbon turnover in coastal wetlands: A global
959 synthesis and perspective. *Earth-Science Reviews*, 218, 103658.
- 960 Zhang, J., Wang, J. J., Xiao, R., Deng, H., & DeLaune, R. D. (2022). Effect of salinity on
961 greenhouse gas production and emission in marsh soils during the decomposition of
962 wetland plants. *Journal of Soils and Sediments*, 1-14.

964

965

966